Heterogeneity of methane seep biomes in the Northeast Pacific

Authors: Sarah Seabrook[1*], Fabio De Leo[2,3], Tamara Baumberger[4], Nicole Raineault[5], Andrew R. Thurber[1,6]

Affiliations:

[1]College of Earth, Ocean, and Atmospheric Sciences, Oregon State University, Corvallis, OR 97331, USA

[2]Ocean Networks Canada, University of Victoria, PO Box 1700 STN CSC, Victoria, BC, Canada V8W 2Y2,

[3]Department of Biology, University of Victoria, PO Box 3080, Victoria, BC, Canada V8W 2Y2

[4]National Oceanic and Atmospheric Administration, Pacific Marine and Environmental Laboratory, Newport, OR 97365, United States

[5]Ocean Exploration Trust, Narragansett, RI 02882, United States

[6]Department of Microbiology, College of Science, Oregon State University, Corvallis, OR 97331, USA

* Corresponding Author: seabroos@oregonstate.edu

Abstract:

Methane seeps provide biogeochemical and microbial heterogeneity in deep-sea habitats. In the Northeast (NE) Pacific Ocean recent studies have found an abundance of seeps at varying spatial separations and within distinct biogeochemical environments ranging in oxygen, depth, and temperature. Here, we examine 8 newly discovered seeps and 2 known seeps covering 800 km and varying across 2000m water depth to identify: (1) novel megafaunal communities in this

geographical region; (2) variations in the microbiome of seep habitats across the margin; (3) spatial and biogeochemical drivers of microbial diversity at seeps. In addition to authigenic carbonates, clam beds, microbial mats, and exposed hydrates - we also observed Siboglinidae tube worm bushes and an anomalous deep-sea barnacle adding to the overall habitats known from the NE Pacific. The microbial communities showed high variability in their spatial distribution and community structure. The seep communities formed distinct groups that included multiple groups of anaerobic methane oxidizing Archaea (ANME; 1, 2ab, 2c, and 3), often co-occurring within one site – however, there were also other sites with clearly dominant members (e.g. ANME-1s at Nehalem Bank). Sulfide oxidizers were dominated by the non-mat forming Campylobacterales and even though vertical gradients in redox potential typify seep sediments, in two cases there was not a significant change in community structure across the top 5cm of sediment. We posit that these patterns were driven by 'bubble-turbation,' and bioirrigation by megafauna. A surprising latitudinal trend was observed in species diversity and richness with increasing richness significantly correlated to increasing latitude. Overall, our results demonstrate that heterogeneity is ubiquitous in the seep biome, spanning all faunal classes, and that the understanding of seeps and the drivers of the community structure can be improved by studying seeps at a range of spatial scales.

1. Introduction

Cold seep habitats are increasingly recognized for their ubiquity in the world's oceans (Brothers et al., 2013; Grupe et al., 2015; Johnson et al., 2015; Levin, 2005). Resulting from the upward advection of hydrocarbons through the sediment, seeps are important sources of energy and heterogeneity in many marine environments (Guilini et al., 2012; Levin and Sibuet, 2012). In

these habitats, chemosynthetic microbial communities convert released hydrocarbons into energy that supports the surrounding ecosystem (summarized in Levin et al., 2016). Abiotic factors (i.e. fluid flux and composition) shape the microbial community (Knittel and Boetius, 2009; Sahling et al., 2002) which, in turn, structures the distribution of the associated macro- and megafauna (Cordes et al., 2010; Levin, 2005). A diversity of chemosynthetic production occurs within the sediment including: (1) the anaerobic oxidation of methane (AOM) carried out by Archaea belonging to the "ANME" group in consortia with sulfate-reducing bacteria (SRB; Knittel and Boetius, 2009; Orphan et al., 2001); (2) sulfide oxidation (thiotrophy) by mat forming microbes (i.e. *Beggiatoa* and *Thioploca)* and non-mat forming linages (i.e. Campylobacterales); and (3) aerobic methane oxidation performed by Gammaproteobacteria (Valentine, 2011). The distribution of these microbial taxa is thought to be driven by the rate of fluid flow from the subsurface (methane supply), which also impacts the metazoans present, including clam and Siboglinidae beds (Bernardino and Smith, 2010; Boetius and Suess, 2004). Recent studies have found methane to be deterministic in the composition of the microbial community in comparison with non-seep habitats (Ruff et al., 2016).

Patterns in biogeography have traditionally been thought to be driven by either local environmental factors (e.g. biogeochemistry), historical geologic events (e.g. geographic isolation), or a combination of both. On large spatial scales (10-20 thousand km) the physical distance between microbial communities has been shown to drive the community structure, while at intermediate spatial scales (10-3000 km) both environmental conditions and physical distance structure the community, and at small spatial scales (0.1-0.3km), the environmental conditions are the most deterministic (Martiny et al., 2006). Seep habitats exemplify the effect of

local environmental variables with distinct vertical and horizontal gradients in the microbial community, which are governed primarily by the availability of electron acceptors (Knittel and Boetius, 2009; Lloyd et al., 2010; Ruff et al., 2015). The distinct biogeochemical processes present within seep habitats correlate to distinct indicator taxa (e.g. ANMEs and SRBs) that contrast with cosmopolitan species typically associated with non-seep marine sediments. The cosmopolitan species drive similarities among the microbial communities of marine sediments globally, particularly at the phylum level (Ruff et al., 2015). However, at the class level and lower these indicator taxa create distinctive microbiomes that are found across spatial scales, with suggestion that cold seeps are island-like habitats that do not necessarily fit traditional models of microbial biogeography (Ruff et al., 2015). Recent discoveries on the pervasiveness of seeps across continental margins provides the opportunity to further disentangle the role of spatial separation and fluid flow in structuring the seep microbiome.

The geologic dynamics of the Cascadia Margin are ideal for the formation of seep habitats. This margin is situated on the accretionary wedge that is associated with the Juan de Fuca subduction zone. The geologic setting of this region yields an environment suited for the migration of subsurface gases to the surface (e.g. Torres et al., 2004; Tréhu et al., 1999). Within the past few years, the known areas of seepage on the Cascadia margin have increased from a few to over five hundred (Bell et al., 2017; Johnson et al., 2015). This margin includes sites that have been studied extensively (e.g. Hydrate Ridge; Boetius and Suess, 2004) and have helped shape our current understanding of methane biogeochemistry (e.g. Hinrichs et al., 1999; Marlow et al., 2014; Orphan et al., 2001). Further, this is a region where productivity, seepage, and oxygen gradients are common and have been shown to impact the composition of fauna present in the

93 region (De Leo et al., 2017; Guilini et al., 2012; Levin et al., 2010). More recently, advances
94 made possible by the installation of Ocean Networks Canada's NEPTUNE cabled observatory,
95 have been allowing continuous and long-term monitoring of cold seep environments in Barkley
96 Canyon (Barkley Hydrates) and Clayoquot Slope, sites located ~500 km north from Hydrate
97 Ridge. This, together with the exploration efforts along the rest of the margin, creates an
98 opportunity for us to delve into the complexity of seep environments along the Cascadia Margin,
99 including potential drivers of modulations in seepage and biogeography of seep fauna.
100
101 While we have learned much about the microbial fauna of the Cascadia Margin, most of this has
102 been focused on a few known sites. Here we describe the habitat types, faunal associations, and
103 the microbial communities present at 8 newly discovered seep sites along the margin, as well as
104 at seep and non-seep sites that have being monitored for nearly 6 years in the context of the
105 NEPTUNE cabled observatory. We use these data to ask:
106 1. What 'habitats' are present at the 8 recently discovered seep habitats?
107 2. What is the Cascadia Margin methane seep microbiome?
108 3. How variable is the microbial community among sites?
109 4. Are there any biogeographic patterns that suggest potential drivers of faunal
110 distributions?
111
112 2. Methods
113 2.1. Study sites and sampling:
114 Samples from the Oregon and Washington margins were collected during Cruise NA072 aboard
115 the *E/V Nautilus* which focused on the Cascadia Margin, defined here as the region between 40-

48°N off the west coast of North America. Push core samples (internal diameter 6.4 cm) were taken by the *ROV Hercules* from seep habitats at each of the sites (Table 1, Figure 1). Upon retrieval, cores were extruded, sectioned at 1 cm intervals with the sides of the cores discarded to avoid smearing and frozen at -80˚C. Samples were also collected further north (47—49°N) along the Cascadia Margin off of British Columbia, Canada, and within the long-term seafloor monitoring sites of Ocean Networks Canada's (ONC) NEPTUNE cabled observatory (Barnes 2007). Push core samples of the same internal diameter were collected during two of ONC's yearly maintenance cruises, with *ROV Jason* aboard *R/V TG Thomson* (Cruise TN328, Sept 2015), and *ROV Hercules* aboard *E/V Nautilus* (Cruise NA071, May-June 2016; Table 1). These sediment cores were vertically sectioned at 0-1, 1-2, 2-3, and 3-5 centimeter intervals, and also preserved at -80˚C.

2.2. DNA extraction and 16S rRNA gene amplification

DNA was extracted from 0.25-0.30g of sediment from the vertically sectioned push core samples with the DNeasy PowerSoil Kit (Mobio/Qiagen) following manufacturer's instructions. The V4 region of the 16s rRNA gene was PCR-amplified with 5PRIME HotMasterMix in triplicate with 515fb and 806rb primers that were bi-directionally barcoded to facilitate multiplexed sequencing following the Earth Microbiome Protocol (Caporaso et al. 2012; Apprill et al. 2015). Amplicons were pooled, quantified using a Qbit and cleaned using the Qiaquick PCR purification kit (Qiagen). Bi-directional sequencing was performed on the Illumina MiSeq platform using the V2 chemistry (2x250 bp) at the Center for Genome Research and Biocomputing (CGRB) at Oregon State University.

139 2.3. Microbial community analysis

140 Sequences were aligned, and quality filtered using mothur v39 (Schloss et al., 2011) and
141 Usearch7 (64 bit; Edgar, 2010). Archaeal and bacterial sequences were clustered using QIIME v.
142 1.9.1 at 97% Operational Taxonomic Unit ($OTU_{0.03}$) and assigned by comparison to the Silva
143 v123 database formatted for QIIME (https://www.arb-silva.de/download/archive/qiime/). For
144 complete pipeline see Supplementary Materials. The 16S rRNA gene sequences are archived in
145 the National Center for Biotechnology Information public database under accession SRP107137
146 (https://www.ncbi.nlm.nih.gov/bioproject/PRJNA386387).
147
148 To compare the community composition and structure across the sites we used both univariate
149 and multivariate statistical analyses to visualize and quantify differences in the community
150 structure. Aligned sequences were rarefied to the least abundant quality-filtered sequences per
151 sample after omitting those with uncharacteristically low sequencing success (which was 16,801
152 sequences per sample for this project) after which they were summarized into discrete taxonomic
153 levels on QIIME v. 1.9.1. Bray-Curtis similarity comparisons on log transformed rarified
154 $OTU_{0.03}$'s were used to generate nonmetric multidimensional scaling (nMDS) plots and cluster
155 diagrams which were used to visualize patterns in the community structure. PERmutation
156 Multivariate ANalysis Of VAriance (PERMANOVA, McArdle and Anderson, 2001) was used to
157 identify significant differences among sites, regions, habitat types and sediment vertical
158 fractions. The levels of similarity among samples and groups were measured using the SIMilarity
159 PERrcentage Analysis (SIMPER, Clarke and Warwick, 2001), and species richness, diversity
160 indexes and rarefaction curves were calculated and compared across sites. Multiple regression
161 analysis was used to identify the main drivers diversity. The factors considered in these analyses

were depth, bottom temperature, dissolved oxygen, and latitude. All multidimensional analyses were performed using the software package PRIMER v7 with the PERMANOVA+ add on (Clarke and Gorley, 2015; Anderson et al., 2008).

3.0 Results

3.1. Site descriptions

3.1.1 Juan de Fuca

This seep was found at 150m depth and consisted of numerous patches of white thiotrophic mats (Table 1, Figure 2a). No bubbling was observed *in situ*, although bubble plumes were observed by multibeam. In addition to the mat, there were patches of reduced (black) sediment (*sensu* Ritt et al., 2011) indicative of active methane release from the habitat. No seep-endemic megafauna nor authigenic (seep-derived) carbonates were observed at this site.

3.1.2 Astoria Canyon SW Wall

Two seeps were sampled from the Astoria Canyon region (Figure 1), a shallow one (495m) which was located on the wall of the canyon and a deeper one (see below). The shallow one (Astoria Canyon SW Wall) had dense vesocomyid clam and authigenic carbonates (Figure 2b); the carbonates served as a substrate to macroinvertebrates including cold water corals. Bubble plumes were abundant at this site.

3.1.3. Astoria Canyon

The deeper site at Astoria Canyon, within the oxygen minimum zone (OMZ; 850m, 4.78 µmol/L O_2), had a diversity of seep habitats including pockmarks, tube-dwelling polychaete beds (*sensu* Thurber et al. 2014), microbial mats, exposed hydrates and reduced sediments (Figure 2c). At

185 this site there were also gastropods with what appeared to be thiotrophic bacteria growing on
186 their back. Bubbling was observed at various locations in the canyon, corresponding to multiple
187 plumes in the multibeam data.
188 3.1.4. Nehalem Bank
189 The seep habitats discovered in Nehalem Bank (190m) consisted of sparse microbial mats and
190 episodic bubbling events were also observed. Both white and orange microbial mats (Figure 2d)
191 were found at this location and a persistent oil slick was found on the surface of the water
192 overlying this site.
193 3.1.5 Heceta SW
194 The Heceta SW site (1225m) had a mosaic of dense seep habitats (Figure 2e,f). Habitats present
195 included Siboglindae bushes (of the vestimentiferan type here and throughout) and vesocomyid
196 clam beds, polychaete beds, sparse *Acharax spp.* individuals, as well as distributed authigenic
197 carbonates and pockmarks. The varied seep habitats hosted a diversity of fauna including
198 anemones, sponges, crustaceans, and gastropods. The site also had exposed hydrates and intense
199 bubbling events.
200 3.1.6. Coquille SW
201 The Coquille SW site, within an OMZ (615m, 7.43 µmol/L O_2), included authigenic carbonates,
202 clam beds, and microbial mats (Figure 2g). The clam shells had what appeared to be arborescent
203 foraminifera covering them. Authigenic carbonates were distributed throughout the Coquille SW
204 site and provided substrate for many sessile invertebrates, including cold water corals. Several
205 bubbling events were observed during the exploration of this site.
206 3.1.7 Klamath Knoll

Occurring within an OMZ (735m, 5.27µmol/L O_2), this site consisted of extensive carbonate platforms with sediment channels interspersed and thin sediment layers on top of the authigenic carbonates. Microbial mats (orange and white variations) and clam beds were present, with the clam beds typically occurring within sediment channels. Many cold water coral species, sponges, and anemones were adhered to the abundant authigenic carbonates. A region of intense sporadic bubbling was found on the edge of a carbonate overhang (Figure 2g).

3.1.8 Trinidad Canyon

Although not sampled, the few instances of seep endemic fauna at Trinidad Canyon (2149m) were notable. At this site, we discovered evidence of what appeared to be a largely inactive seep habitats including beds of clam shells and potentially inactive authigenic carbonates. However, we also discovered small beds of live clams, patches of reduced sediment, live Siboglindae bushes, and a live gooseneck barnacle assemblage (Figure 2i). These live assemblages suggested that there was still some degree of methane flowing through the sediment, despite the other areas appearing to be dormant/extinct seeps.

3.1.9 Barkley Canyon

The two sampling sites in Barkley Canyon are located adjacent to the northern flank and at mid portion of the canyon (Fig 1). Barkley Axis, at 987 m, intersects the core of the OMZ offshore Vancouver Island (ranging 6.7-13.4 µmol/L O_2), with the seafloor consisting of a mixture of sandy and muddy sediments and patches of microbial mats. The Barkley Hydrates site, at 870 m, is situated in a 1 km^2 plateau slightly less than a kilometer west from Barkley Axis. A mosaic of exposed hydrate mounds, bacterial mats and muddy sediments compose the seafloor at this location (Thomsen et al., 2012; Chatzievangelou et al., 2016).

3.1.10 Clayoquot Slope

This seep site at a depth of 1250 m (near the bottom of the OMZ with values ranging from 13.4-22.3 µmol/L O_2) is located 20 km landward of the toe of the Cascadia subduction zone, and presents localized and temporally variable methane bubble emissions (Römer et al., 2016). Clam beds (*Calyptogena* spp.), carbonate mounds with the presence of ampharetid polychaete thickets, and high densities of sea pens in conspicuous associations with the ophiuroid *Asteronix loveni* in the area.

3.1.11 Cascadia Basin

In this abyssal site, at 2660 m of depth and ~100 km offshore from the Cascadia subduction zone, the seafloor landscape is typical of abyssal settings with a nearly flat topography and fine grained sediments with very little spatial heterogeneity at 10's of km scales. Local benthic megafauna is mostly constituted of echinoderms (holothurians and seastars), and macrourid fishes.

3.1.12 Endeavour

Located at the northern segment of the medium rate (6 cm/yr) spreading center known as the Juan de Fuca Ridge, the Endeavour vent field is perhaps one of the best-studied vent sites worldwide (Kelley et al., 2012). At 2300m of depth, the sampling site at Endeavour is comprised of a highly three-dimensionally structured habitat with very tall sulfide towers and black smokers, pillow lava and other basaltic rock formations. The core sampled at Endeavour for this project was retrieved from sediment that did not overlay the vents and is considered to be reference sediment.

3.2 Overall trends in the microbial communities

252 A total of 1,663,299 sequences across the 104 samples were used to explore the microbial
253 community structure. This resulted in the identification of 30,652 Bacterial and Archaeal OTU's
254 recovered, with 19.6% belonging to Archaea and the remaining 24,617 OTUs classified as
255 bacteria. The microbial communities identified in this study were most similar (indicated by
256 SIMPER similarity percentages) within regional groupings: Oregon/California Margin seeps
257 (40.6%), British Columbia Seeps (40.8%), and British Columbia reference sites (43.8%) (Figure
258 3). Although there was only one sample from the Washington Margin, it was most similar to the
259 British Columbia seeps (33.7%); the Washington Margin seep was 30% similar to the
260 Oregon/California Margin seeps. There were significant differences among these groupings
261 (PERMANOVA pseudo-F=12.708, $p \leq 0.001$, significance of the pairwise comparisons based on
262 this model are indicated below). The Oregon/California Margin seeps were significantly different
263 from the British Columbia reference sites ($p \leq 0.001$) and the British Columbia seep sites
264 ($p \leq 0.001$) and not significantly different from the Washington Margin seep ($p=0.060$). The
265 British Columbia seep sites were significantly different from the British Columbia reference sites
266 ($p<0.001$) but not significantly different from the Washington Margin sample ($p=0.260$), while
267 the British Columbia reference sites were significantly different from the Washington Margin
268 sample ($p=0.040$).
269
270 Within the aforementioned regional groupings, the microbial community structure was
271 significantly different between the different habitat types (clam bed vs. microbial mat) of the
272 Oregon/California and Washington Margin seep sites (PERMANOVA, pseudo-F=11.41,
273 $p \leq 0.001$, Figure S1). We were unable to test the role of habitat in structuring the community at
274 other locations, due to limited samples for comparison of both habitats at a given site. There

were also significant differences between the vertical fractions of sediment sampled (pseudo-F=2.00, $p < 0.001$, Table S1). The pairwise comparison based on this model revealed no differences among vertical fractions that were next to each other (i.e. 1-2cm and 2-3cm; $p > 0.050$) however there was a significant difference between those samples that were most separated vertically (i.e. 0-1 cm and 4-5 cm, and 0-1 cm and 3-5 cm; $p < 0.003$).

Surprisingly, there was an apparent decrease in species richness from north to south (Figure 4). To quantify what factors may be driving this pattern, we utilized a multiple regression analysis including depth, oxygen saturation, temperature and latitude as explanatory variables. This identified that latitude best explained this pattern of OTU richness, solely explaining 29% of the variance ($r^2=0.29$, $p < 0.001$). All of the other factors except for oxygen correlated with each other and latitude so, due to concerns of co-variance, were thus excluded from further analysis. This covariance should be kept in mind when considering latitude as a driver of variance. Oxygen did not significantly increase the fit of the model. Exploring trends in the microbial community further with a multiple regression analysis based on the Shannon Diversity indexes for the samples and including the aforementioned variables revealed both latitude and oxygen concentration as the drivers of variance in OTU diversity. Notably, latitude ($p < 0.001$) was again the most significant driver, explaining 22% of the variance, while latitude and oxygen saturation ($p=0.006$) together explained 30% of the variance.

3.3 Microbial community composition

The abundances of the top 19 bacterial Orders varied among sites with the most obvious differences between the groupings of Oregon Margin seep sites, Washington Margin seep site,

British Columbia seep sites, and British Columbia reference sites (two-way crossed ANOSIM; $r_{spearman}$= 0.87, $p_{spearman} \leq 0.001$; Figure 5). Within the Oregon and Washington Margin seep sites, the order Desulfobacterales was the most dominant, making up 20±1.5% (±SE here and throughout) of the community composition. SRB's *Desulfobulbus*, *SEEP-SRB1,* and *SEEP-SRB2* were the main taxa within the Desulfobacterales at the Oregon margin seep sites comprising 6±1.0%, 4±0.5%, 1±0.5% of the relative abundance, respectively. Camplyobacterales (*Sulfurovum* (4±0.4%) and *Sulfurimonas* (2±0.4%), Thiotrichales (4.9±0.5%), Chromatiales (2.5±0.2%), Anaerolineales (2.3±0.3%), and Methylococcales (2.3±0.3%) were also abundant. In the sample from the Washington margin Xanthomonadales was the most abundant bacteria at 8% along with the Deltaproteobacteria Sh765B-TzT-29 (6.7%), Myxococcales (6.6%), Methylococcales (5.9%), Cellvibrionales (5.6%), and Desulfobacterales (4.4%).

At the British Columbia reference sites, Xanthomonadales was the most abundant bacteria observed making up 11.7±0.4% of the community. The Deltaproteobacteria Sh765B-TzT-29 was the next most abundant at the non-seep sites (6.5±3% of the community). Brocadiales (associated with Anaerobic Ammonia Oxidation [ANNAMOX]; 6.4±0.7%), Rhodospirillales (5.5±0.2%), and Chromatiales (2.8±0.3%) were also abundant.

In the British Columbia seep samples, Deulfobacterales was the most abundant at 8.5±0.7% followed by Xanthomonadales (6.8±0.6%), the Deltaproteobacteria Sh765B-TzT-29(6.2±0.5%), and Brocadiales (3.6±0.2%). There is variation with in this overall trend, however, particularly with the core that was taken from an area that appeared to be experiencing the greatest seep input (i.e. black sediment indicative of a reduced environment) that was sampled at Clayoquot Slope,

where Campylobacterales increases in abundance throughout the core to 11.5% of the relative abundance at 3-5cm, despite averaging 0.9±0.5% for the British Columbia seep samples overall.

The most dominant Archaea were those normally associated with methane seep and benthic habitats with the orders ANME, Woesearchaea, Marine Group I, Thermoplasmata, and Marine Benthic Group B dominating (Figure 6). The phylum Woesearchaea was the most abundant in the Washington Margin seep site, British Columbia seep sites, and British Columbia reference samples ranging from 4.0% of the microbial community at Cascadia Basin to 0.5% at the Juan de Fuca seep. The seep sites off of Oregon/California had ANME-1 as the most abundant Archaeal taxa, for which they composed 3.7±1.3% of the community composition. Some of these sites had co-occurrences of all ANME types whereas others had just one ANME group dominating.

3.4 Vertical patterns in the abundance of key players in the seep microbiome of the Oregon Margin

3.4.1 Anaerobic methane oxidizers (ANME)

The distribution of ANME varied among sites in its composition and vertical distribution (Figure 7). ANME-1b dominated, composing 5±3.5% of the microbial community at 5 cm sediment depth, in both cores from Astoria Canyon SW Wall (Cores A and B). However, in Astoria Canyon SW Wall-B, ANME-2ab (2.7%) and ANME-1 (2.2%) were also present below 2-3 cm. Although ANME-1's did not dominate between 0 and 5 cm in the Nehalem Bank cores (Cores A and B), ANME-1a was present at 3-4 cm with a peak of 4.2% in Nehalem Bank-B. Only Nehalem Bank-A was sequenced below 5 cm and it showed an impressive dominance of

ANME-1 peaking at 52% of the microbial community at 8-9 cm depth. Klamath Knoll was largely dominated by ANME-1a, with a sharp peak of 12.3% at 3-4 which coincided with a small peak of 2% in ANME-1.

While ANME-1 appeared to dominate the ANME community in certain cores, others had abundant ANME-2 lineages that showed differential depth distributions. For example, the ANME community between 0 and 5 cm at Nehalem Bank (Cores A and B) was dominated by ANME-2ab with a peak at the 4-5 cm depth (4.4±3.4%). In addition, Astoria Canyon and Coquille SW samples had both ANME-2ab and ANME-2c increasing throughout the top 5 centimeters of sediment with ANME-2ab the most dominant (0.7% and 0.8%, respectively). Astoria Canyon also had a peak (0.2%) in the relative abundance of ANME-3 at 3-4 cm, but it was not dominant. The core sampled at Heceta SW had low overall relative abundance of ANME, however the ANME community that was present was dominated by ANME-3 with a peak at 3-4 centimeters depth, albiet at a low relative abundance (0.025%) of the microbial community; this contrasted with the other sites where ANME-2 and ANME-1 lineages dominated.

3.4.2 Sulfate Reducing Bacteria (SRB)

Deltaproteobacteria associated with sulfate reduction, which are in many cases known to be the syntrophic partners of ANME, followed similar trends of clear changes in vertical distributions and among site variance in composition (Figure 8). Desulfobulbus, comprising an average of 6.8±1.0% of the relative abundance of the microbial community, was the most dominant SRB in the 0-3 cm range at all sites, continuing to be the most dominant down to 5 cm at Astoria Canyon

(peak at 3-4 cm of 15%), Heceta SW (peak at 2-3 cm of 7.8%), and Coquille SW (peak at 3-4 cm of 4.5%). After 3-4 cm in Astoria Canyon SW Wall (Cores A and B), SEEP-SRB1 becomes the most dominant SRB at 10±1.0% relative abundance. This is coupled with an increase in both Desulfococcus and SEEP-SRB2 after 2-3 cm to 2.8% and 3.7%, respectively, in Astoria Canyon SW Wall-B. Similarly, in Nehalem Bank (Cores A and B), SEEP-SRB1 increases in relative abundance after 3-4 cm to 5.8±2.6% at 4-5 cm concurrent with an increase in Nehalem Bank-B of Desulfococcus (1.8%) and SEEP-SRB2 (1.5%) to 4-5 cm. Desulfococcus also increases in Nehalem Bank-A to 7% of the relative abundance at 5 cm, and SEEP-SRB2 - although making up only 0.6% of the microbial community at 4-5 cm, increases to 26% of the relative abundance at 5-6 cm. Seep-SRB1 dominates in the Klamath Knoll core, reaching a maximum relative abundance of 11% at 4-5cm. Desulfobulbus decreases throughout the 0-5cm from 2% to 0.5% of the relative abundance in the Klamath Knoll core and SEEP-SRB2 increases from 0.01% to 2.6%, respectively.

3.4.3 Sulfide Oxidizing Bacteria

The sulfide-oxidizing Thiotrichales (mat-forming) order and the *Sulfurovum* (non-mat forming) genera also showed differential trends in their vertical distribution in the Oregon/California Margin seep samples (Figure 5). At Astoria Canyon SW wall (Cores A and B), Thiotrichales decreased in relative abundance from 5.7±0.5% of the microbial community at 0-1 cm depth to 2.8±0.01% at 4-5 cm depth. Similarly at Nehalem Bank (Cores A and B) and Astoria Canyon, Thiotrichales decreased from 18.8±0.6% and 3.4% at 0-1 cm to 2.7±0.8% and 2.0% at 4-5cm, respectively. Divergent from this, at Heceta SW and Coquille SW, Thiotrichales increased in relative abundance from 4.3% and 2.6% of the microbial community at 0-1cm to 7.4% and 6.7%

390 at 4-5 cm. There were no clear trends in the relative abundance of Thiotrichales at Klamath
391 Knoll. At Nehalem Bank (Cores A and B) and Astoria Canyon, *Sulfurovum* increased in relative
392 abundance from 0.6±0.2% and 1.5% at 0-1cm to 5.9±1% and 3.4% at 4-5 cm, respectively.
393 Similarly, *Sulfurovum* increased in relative abundance as well at Heceta SW from 2.7% at 0-1cm
394 to 4.1% at 4-5 cm. However, at Coquille SW and Klamath Knoll, *Sulfurovum* decreased in
395 relative abundance from 13.7% and 3.0% of the relative abundance at 0-1 cm to 2.9% and 0.8%
396 at 4-5 cm, respectively.
397
398
399 4. Discussion
400
401 4.1 Overall patterns in distribution and abundance:
402 A range of seep habitats were observed throughout the explorations of the Cascadia Margin. This
403 included: microbial mats (both orange and white variations), clam and tube-dwelling polychaete
404 beds, siboglinid assemblages, and sparse instances of *Archarax* spp. and gooseneck barnacles.
405 The heterogeneity within and among seep biomes is highlighted by this variation in the observed
406 megafaunal assemblages. Notable is the discovery of vestimentiferan siboglinids at Heceta SW
407 and Trinidad Canyon, adding to the limited reports of this group within seep habitats in the NE
408 Pacific (see Bernardino and Smith, 2010; Grupe et al., 2015; Kulm et al., 1986). The discovery
409 of vestimentiferans at Heceta SW was particularly interesting because of the similarity of this
410 habitat to Hydrate Ridge and Eel River Basin, which occur in areas that also experience lower
411 oxygen concentrations associated with the OMZ and have been extensively explored but
412 conspicuously lack vestimentiferan siboglinids (Levin et al., 2010). One guiding hypothesis on

why these taxa do not occur at Eel River Basin and Hydrate Ridge has been that they both occur within or near the upper bounds of the OMZ and low oxygen has been suggested to exclude vestimentiferans (and bathymodiolin mussels) from these locations. While this may be the case for why the vestimentiferans are present at Trinidad Canyon, a site that is well below the permanent OMZ (56.90 µmol/L O_2), Heceta SW lies just below the most intense core of the OMZ and has hypoxic conditions (16.26 µmol/L O_2). Eel River Basin methane seep occurs slightly shallower than Heceta SW and in even more normoxic water, making the occurrence of vestimentiferan siboglinids at Heceta SW surprising and challenging the notion that oxygen concentration alone drives the lack of vestimentiferan siboglinids. The discovery of gooseneck barnacles at Trinidad Canyon was also notable as the gooseneck barnacles include groups that are vent-endemic with interesting biogeographical and evolutionary distributions (Herrera et al., 2015) but are not common members of methane seeps (but see Yamaguchi et al., 2004). Large gooseneck barnacles do include non-reducing habitat groups as well. While it is unclear whether the one we observed is a previously unknown seep endemic, or just a deep-sea species taking advantage of the hard substrate provided by the Siboglinidae tubes, this increases the fauna known to inhabit seeps in this region.

Seep communities are a result of both the current and historic dynamics of the region with multiple successional patterns proposed. Consequentially, fluid flow rate and duration of seepage can influence the fauna present. At many seep systems the rate of fluid flow is thought to drive the patterns of fauna (e.g. Bernardino et al., 2010; Sahling et al., 2002). Microbial mats occur in areas of higher methane and sulfide flux whereas clam beds have lower or oscillating flow regimes (Tryon et al., 2002) and Siboglinidae's are intermediate in their flux regime

436 (summarized in Bernardino et al., 2010). Taxonomic distribution may also be driven by
437 successional stages of a seep in addition to seepage rate. It has been posited that upon the onset
438 of seepage, microbial mats appear which are then replaced by clam beds and/or siboglinid
439 assemblages as the seep matures. As the seepage continues, authigenic carbonates form as a
440 byproduct of the anaerobic oxidation of methane that in turn provide substrate for background
441 communities (Bowden et al., 2013; Cordes et al., 2009). Thus the extent and rate of seepage can
442 both lead to similar patterns of fauna. While this presents a challenge for interpreting certain
443 faunal groups in seep habitats others are more clear. For example, habitats that had a diversity of
444 seep habitats (defined by the fauna present) and that had extensive carbonate features (i.e. Heceta
445 SW, Astoria Canyon sites, Coquille SW, and Klamath Knoll) are likely seeps that have been
446 persistent for long time periods and/or experience sustained and higher flow than others. In
447 contrast sites with mostly microbial mats (i.e. Juan de Fuca and Nehalem Bank) may either be
448 relatively recent features or experience lower flux that does not lead to the development of more
449 expansive or diverse habitats.
450
451 Another surprising trend was that many of the taxa that are often found as dominant in seeps co-
452 occurred to a greater extent than previously expected and a few taxa were more dominant than
453 expected. Particularly, the different ANME lineages often co-occur but one dominates (Knittel
454 and Boetius, 2009). Here we observed some of the sites with extreme dominance (e.g. Nehalem
455 Bank and ANME-1) and other sites where there was a more even distribution (Astoria Canyon
456 SW Wall). Additionally, ANME-2 lineages have been shown to be dominant at other known
457 seeps in the region (i.e. Hydrate Ridge; Knittel and Boetius, 2009) and although we observed this
458 at some sites, in many instances ANME-1 lineages comprised the majority of the ANME present.

459 Further ANME- 3, often found in mud volcanoes, was present at some of our sites, including
460 being the dominant ANME type at Heceta SW (albeit at a low total percentage of the microbial
461 community). The spatial scale and survey approach taken here can help us understand the
462 distribution of microbial taxa and both further refine and augment distribution patters (such as
463 those proposed by Ruff et al. 2014).
464 4.2 Small scale variability
465 Methane seeps are an area with large gradients in the biogeochemical composition over small
466 vertical spatial scales within the sediment. The sediment has often become anoxic within the
467 first mm of the sediment and sulfate concentrations can approach zero within the top few cm of
468 sediment in areas of high seepage. These steep chemoclines lead to niche specification within
469 the microbial community (Boetius and Suess, 2004; Cordes et al., 2010; Macalady et al., 2008).
470 The sulfide oxidizing groups of bacteria are thought to be influenced by these steep chemoclines
471 (Pjevac, 2014). Microbial mats, most often dominated by Thiotrichales of the generas *Beggiatoa*
472 and *Thioploca*, have been found to be more prominent in diffusive controlled niches with high
473 sulfide/oxygen levels and are often most abundant at the sediment surface (Macalady et al.,
474 2008). This contrasts with *Sulfurovum* and other Camplyobacerterales types that are thought to
475 dominate in areas of increased sulfide flux and lower concentrations of oxygen, sometimes even
476 using nitrate rather than oxygen as the electron acceptor (Grünke et al., 2011; Nguyen, 2016;
477 Pjevac, 2014). Within the microbial mats at the Cascadia Margin seeps, we found Thiotrichales
478 to be more abundant in the surface sediment with the Camplyobacterales (i.e. *Sulfurovum*
479 another sulfide oxidizing group*),* more dominant in deeper sediment layers. Thus the distribution
480 of Thiotrichales and Camplyobacterales observed at out sites fit the distribution patterns found

481 elsewhere, with Thiotrichales dominating the surface and better oxygenated regions with the
482 Camplyobacterales found deeper in the sediment.
483
484 Clam beds, which often have a sulfide peak at or below 4 cm depth in the sediment, were present
485 at Astoria Canyon SW Wall, Heceta SW, Coquille SW and Klamath Knoll (Sahling et al., 2002;
486 Valentine et al., 2005). At these sites *Sulfurovum* was found to increase with depth down to 5
487 cm, except from at Coquille SW and Klamath Knoll where *Sulfurovum* decreased from 0-1 cm to
488 4-5 cm. The core from Klamath Knoll was taken from a clam bed within a sediment filled
489 channel, a physically different environment than the other clam beds sampled. This potentially
490 contributed to its divergence in community structure, and in the abundance of *Sulforovum,* due to
491 the hydrodynamics caused by the adjacent carbonate outcrops. Another core that had a unique
492 vertical distribution of the microbial community compared to the other cores was a core that was
493 collected from a clam bed in Coquille SW. The uniqueness of this core could have been partially
494 driven by what appeared to be aborescent foramnifera growing on clam shells and tufts of
495 microbial mat distributed throughout the bed. The presence of protists such as aborescent
496 foramnifera in seep environments has been shown to increase habitat heterogeneity and
497 contribute to carbon cycling (Pasulka et al., 2017). The marked difference in the microbial
498 community between this core, collected from a clam bed, and the others sampled in clam beds
499 was indicated with a greater similarity of this core to other cores collected from microbial mats at
500 0-1 cm (Figure S1). In this particular case it is difficult to disentangle if the abundance of the
501 protists is driving this or if the protists are a result of the biogeochemistry of the environment.
502

503 Both the Astoria Canyon core and the Heceta SW core showed little vertical trend in abundance
504 in microbial taxa. The Astoria Canyon core, taken from a dense microbial mat, was from an area
505 of significant bubbling and surrounded by exposed hydrates. Likely, in this core, the lack of a
506 clear vertical trend with the microbial community was due to 'bubble-turbation' of the sediment.
507 This is similar to what occurs at mud volcanoes such as the Håkon Mosby Mud Volcano
508 (HMMV), where sediment mixing alters the microbial community in the surface sediment
509 (Lösekann et al., 2007). Unlike HMMV, aerobic methanotrophs did not comprise >50% of the
510 microbial community in this site (maximum of 11.5% of total microbial community), which may
511 reflect the lower availability of oxygen within overlying water (Table 1). The high abundance of
512 SRBs and ANMEs within the top few cms of sediment also suggest that oxygen penetration was
513 limited within the Astoria Canyon microbial mat sampled. The other location that showed a
514 similar trend was from a clam bed at Heceta SW with large clams present; there were also a few
515 siboglinids within the sediment. Clams both bioirrigate and bioturbate the sediment (Wallmann
516 et al., 1997), potentially smearing biogeochemical gradients, and often occur in areas where there
517 is fluid flow both into and out of the sediment (Orphan et al., 2004; Tryon et al., 2002, 1999). So
518 unlike the Astoria canyon core that we posit is bubble-turbated, the faunal turbation at this site
519 likely led to the absence of a clear vertical trend with the microbial community within the top 5
520 cms. Further, sulfate leakage from the roots of siboglinids has been shown to occur, a process
521 which stimulates the anaerobic oxidation of methane around the root area (Cordes et al., 2005,
522 2003). Thus the presence of siboglinids could have been removing vertical gradients and creating
523 horizontal gradients, as a result of both the sulfate leakage from the roots, leading to horizontal
524 rather than vertical chemoclines and the more 'smeared' structure of the microbial community at
525 Heceta SW.

526

527 4.3 Biogeographic patterns

528 A surprising trend was the latitudinal gradient in seep microbial community. While we were
529 unable to heavily replicate sampling from within any one site our approach did allow us to
530 collect a snap shot of the microbial community across significant spatial scales and
531 environments. The sites ranged in depth from 190 m to 2149 m (Table 1 and 2), spanned 800 km
532 of latitude, and varied from sparse microbial mats to massive hydrate outcrops with extensive
533 bubble emission. While on a fundamental level, this highlights the diversity of seep habitats and
534 dynamics on the margin, it also allowed a holistic view of the seepage beyond one particular site,
535 complimenting those studies that provide high resolution at a site-level spatial scale. With this
536 approach we found that there were significant shifts in the community composition going from
537 the sites off Vancouver Island to the more southerly sites.

538

539 The composition of seep communities studied here were dominated by SRBs, methanotrophs,
540 and sulfate oxidizing bacteria while the non-seep sites were dominated by cosmopolitan bacteria
541 associated with deep-sea sediments. While the role of seepage rates, successional patterns, and
542 background fauna have been used to explain overall patterns of diversity in seep sediments in the
543 past, the results here add to this by suggesting that large scale latitudinal trends may have an
544 overarching influence on these previously observed patterns. Previous studies have described
545 increased diversity and species richness of macrofauna in non-seep sites, with this observation
546 attributed often to higher niche specification of seep communities (Grupe et al., 2015). This is in
547 contrast to our findings, as we observed increased diversity of microbial taxa at seep compared to
548 our reference sites.

549

550 Here, variance of both species richness and diversity with latitude suggest that latitude may be a
551 driver in the composition and richness of the methane seep microbiome. The additional variance
552 of diversity with oxygen saturation highlights the potential impact that variations in oxygen
553 saturation, observed in areas such as OMZ, could have upon microbial communities. Together,
554 this supports previous work indicating impacts on the heterogeneity of marine environments
555 from variations in oxygen saturation (such as in OMZs; Guilini et al., 2012; Pasulka et al., 2016),
556 while also revealing a potential new driver of community composition in seep microbiomes. We
557 would like to point out that in some cases the areas sampled as seep habitats within the ONC
558 array system off Vancouver Island did not appear to experience the same extent of seepage as
559 those sampled more southerly, even though very active seep sites do occur in within the ONC
560 sites. They were, however, very clearly seep habitats as ANME were present, and importantly, if
561 one omits all of the British Columbia samples from the analysis there is still a latitudinal trend
562 (Figure 4). Additional focused surveying efforts along the NE Pacific margin would help to
563 further elucidate these possible trends in seep biogeography.
564

565 Intriguing trends in biogeographic patterns of reducing habitat communities are beginning to
566 identify large scale patterns in species composition and diversity in microbial (Ruff et al., 2015)
567 and animal communities (Bachraty et al., 2009; Van Dover et al., 2002). Biogeography of the
568 deep sea is thought-provoking due to the dispersal mechanisms of fauna that must coexist with
569 slow water movements, cold but stable temperatures, and low food supply. Reducing habitats in
570 this context serve as additional disparate islands that aid in the survival of fauna leading to
571 patterns where distance and chemical similarity have resulted in interesting constructs of the

572 mechanisms that communities use to disperse. The patterns and explanations of biogeography in
573 deep-sea macro- and megafauna communities are interesting (Baco et al., 1999; Herrera et al.,
574 2015; Hilario et al., 2015) and microbial communities have also been identified as having clear
575 biogeographic and seasonal patterns in their distribution and composition (Ladau et al., 2013;
576 Ruff et al., 2015). To understand the factors that drive these patterns of observed species
577 distributions, sampling needs to occur on nested scales where similarity at different distances and
578 the factors that drive those (or add to them) are quantified. Here, we have added to the overall
579 understanding of large scale faunal distributions, adding to limited reports of siboglinids in the
580 NE Pacific and the discovery of the gooseneck barnacle that may or may not be a seep endemic.
581 Further, we have quantified both regional and local variability of the microbial community in
582 seep habitats, contributing to important global comparisons that exist (i.e. Ruff et al. 2015).
583
584 5. Conclusions
585 Select seep habitats in the NE Pacific have been heavily studied (Hydrate Ridge, Eel River
586 Basin), but we are just beginning to appreciate the extent and variability of seepage in the NE
587 Pacific. Seeps are important to global carbon cycling, energy flow, and overall functioning of the
588 earth system (Brooks et al., 2017; Sweetman et al., 2017; Thurber et al., 2014; Levin et al. 2016).
589 In just two years, directed study of the continental margin off of Washington, Oregon, and
590 Northern California resulted in >500 individual bubble plumes (Bell et al., 2017). The seep
591 habitats discovered in this study covered a range of depths (150m to 2149m), latitudes, and
592 oxygen concentrations. In addition to the microbial mats, authigenic carbonates and vesicomyid
593 clam beds that are known in the NE Pacific, we also observed siboglinid tubeworm assemblages
594 in a habitat that intersects the top of the OMZ and is similar to well-studied seep habitats (Eel

River Basin and Hydrate Ridge) in which they have not been found. We found significant differences in the microbial community composition between regional groupings, habitat type (microbial mat vs. clam bed), and vertical fraction within the sediment. Trends in species richness were driven by changes in latitude while observed variance in diversity were driven by both latitude and oxygen concentration. This compliments previous studies where the main drivers of the seep microbial community were seafloor temperature and electron acceptor availability (Ruff et al., 2015). This study highlights the variability and complexity that exists within seep communities of the NE Pacific. This also presents a framework for further studies of seep habitats as it provides an overview of additional sites and variance in community structure that can be used to more comprehensively constrain how fluid flow, chemical, physical and geological dynamics, and geographic location contribute to the composition and functioning of seep ecosystems, beyond particular sites.

Acknowledgements:

We would like to thank R. Embley, S. Merle, and the Captains and crew of the NA072 cruise aboard the E/V *Nautilus*. Cruise NA072 was operated by the Ocean Exploration Trust Inc. and funded by the NOAA Office of Exploration and Research. We also thank the Canada Foundation for Innovation for ship and ROV time devoted to the collection of push core samples during two of Ocean Networks Canada-NEPTUNE observatory maintenance cruises (TN328, NA071). We are indebted to the generosity of ONC in providing samples to facilitate this study and we particularly thank K. Douglas for assembling the final layout for the basemap in Figure 1. A portion of S. Seabrook's time in the preparation of this manuscript was supported by the U.S. National Science Foundation, Office of Polar Programs 1642570 award to A.R. Thurber. A

618 portion of this project was supported by the International network for scientific investigation of
619 deep-sea ecosystems (INDEEP) supported by Foundation Total. This work is under PMEL
620 contribution number 4673.
621
622
623
624
625
626
627
628 References
629 Anderson, M.J., Gorley, R.N., Clarke, K.R., 2008. PERMANOVA+ for PRIMER: Guide to
630 Software and Statistical Methods. PRIMER-E, Plymouth, UK.
631 Bachraty, C., Legendre, P., Desbruyères, D., 2009. Biogeographic relationships among deep-sea
632 hydrothermal vent faunas at global scale. Deep. Res. Part I Oceanogr. Res. Pap. 56, 1371–
633 1378. doi:10.1016/j.dsr.2009.01.009
634 Baco, A.R., Smith, C.R., Peek, A.S., Roderick, G.K., Vrijenhoek, R.C., 1999. The phylogenetic
635 relationships of whale-fall vesicomyid clams based on mitochondrial COI DNA sequences.
636 Mar. Ecol. Prog. Ser. 182, 137–147. doi:10.3354/meps182137
637 Bell K.L.C., J. Flanders, A. Bowman, N.A.R., 2017. New Frontiers in Ocean Exploration: The
638 E/V Nautilus, NOAA Ship Okeanos Explorer, and R/V Falkor 2016 field season.
639 Oceanography 30, 94. doi:10.5670/oceanog.2016.supplement.01
640 Bernardino, A.F., Smith, C.R., 2010. Community structure of infaunal macrobenthos around

641 vestimentiferan thickets at the San Clemente cold seep, NE Pacific. Mar. Ecol. 31, 608–621.
642 doi:10.1111/j.1439-0485.2010.00389.x
643 Boetius, A., Suess, E., 2004. Hydrate Ridge : a natural laboratory for the study of microbial life
644 fueled by methane from near-surface gas hydrates 205, 291–310.
645 doi:10.1016/j.chemgeo.2003.12.034
646 Bowden, D.A., Rowden, A.A., Thurber, A.R., Baco, A.R., Levin, L.A., Smith, C.R., 2013. Cold
647 Seep Epifaunal Communities on the Hikurangi Margin, New Zealand: Composition,
648 Succession, and Vulnerability to Human Activities. PLoS One 8.
649 doi:10.1371/journal.pone.0076869
650 Brooks, J.M., Kennicutt, M.C., Fisher, C.R., Macko, S.A., Cole, K., Bidigare, R.R., Vetter, R.D.,
651 2017. Deep-Sea Hydrocarbon Seep Communities : Evidence for Energy and Nutritional
652 Carbon Sources Published by : American Association for the Advancement of Science
653 Stable URL : http://www.jstor.org/stable/1700859 REFERENCES Linked references are
654 available on JS 238, 1138–1142.
655 Brothers, L.L., Dover, C.L. Van, German, C.R., Kaiser, C.L., Yoerger, D.R., Ruppel, C.D.,
656 Lobecker, E., Skarke, A.D., 2013. Evidence for extensive methane venting on the
657 southeastern U . S . Atlantic margin 807–810. doi:10.1130/G34217.1
658 Cordes, E.E., Bergquist, D.C., Fisher, C.R., 2009. Macro-ecology of Gulf of Mexico cold seeps.
659 Ann. Rev. Mar. Sci. 1, 143–168. doi:10.1146/annurev.marine.010908.163912
660 Cordes, E.E., Bergquist, D.C., Shea, K., Fisher, C.R., 2003. Hydrogen sulphide demand of long-
661 lived vestimentiferan tube worm aggregations modifies the chemical environment at deep-
662 sea hydrocarbon seeps. Ecol. Lett. 6, 212–219. doi:10.1046/j.1461-0248.2003.00415.x
663 Cordes, E.E., Cunha, M.R., Galéron, J., Mora, C., Olu-Le Roy, K., Sibuet, M., Van Gaever, S.,

664 Vanreusel, A., Levin, L.A., 2010. The influence of geological, geochemical, and biogenic
665 habitat heterogeneity on seep biodiversity. Mar. Ecol. 31, 51–65. doi:10.1111/j.1439-
666 0485.2009.00334.x
667 Cordes, E.E., Hourdez, S., Predmore, B.L., Redding, M.L., Fisher, C.R., 2005. Succession of
668 hydrocarbon seep communities associated with the long-lived foundation species
669 Lamellibrachia luymesi. Mar. Ecol. Prog. Ser. 305, 17–29. doi:10.3354/meps305017
670 Edgar, R.C., 2010. Search and clustering orders of magnitude faster than BLAST. Bioinformatics
671 26, 2460–2461. doi:10.1093/bioinformatics/btq461
672 Grünke, S., Felden, J., Lichtschlag, A., Girnth, A., De Beer, D., Wenzhöfer, F., Boetius, A.,
673 2011. Niche differentiation among mat-forming, sulfide-oxidizing bacteria at cold seeps of
674 the Nile Deep Sea Fan (Eastern Mediterranean Sea). Geobiology 9, 330–348.
675 doi:10.1111/j.1472-4669.2011.00281.x
676 Grupe, B.M., Krach, M.L., Pasulka, A.L., Maloney, J.M., Levin, L.A., Frieder, C.A., 2015.
677 Methane seep ecosystem functions and services from a recently discovered southern
678 California seep. Mar. Ecol. 36, 91–108. doi:10.1111/maec.12243
679 Guilini, K., Levin, L.A., Vanreusel, A., 2012. Progress in Oceanography Cold seep and oxygen
680 minimum zone associated sources of margin heterogeneity affect benthic assemblages ,
681 diversity and nutrition at the Cascadian margin (NE Pacific Ocean). Prog. Oceanogr. 96,
682 77–92. doi:10.1016/j.pocean.2011.10.003
683 Herrera, S., Watanabe, H., Shank, T.M., 2015. Evolutionary and biogeographical patterns of
684 barnacles from deep-sea hydrothermal vents. Mol. Ecol. 24, 673–689.
685 doi:10.1111/mec.13054
686 Hilariio, A., Metaxas, A., Gaudron, S.M., Howell, K.L., Mercier, A., Mestre, N.C., Ross, R.E.,

687 Thurnherr, A.M., Young, C., 2015. Estimating dispersal distance in the deep sea: challenges
688 and applications to marine reserves. Front. Mar. Sci. 2, 1–14.
689 doi:10.3389/fmars.2015.00006
690 Hinrichs, K., Hayes, J.M., Sylva, S.P., 1999. Methane-consuming archaebacteria in marine
691 sediments 398, 802–805.
692 Johnson, H.P., U.K. Miller, M.S. Salmi, and E.A.S., 2015. Analysis of bubble plume
693 distributions to evaluate methane hydrate decomposition on the continental slope. Geochem.
694 Geophys. Geosyst 3825–3839. doi:10.1002/2015GC005955.Received
695 Knittel, K., Boetius, A., 2009. Anaerobic oxidation of methane: progress with an unknown
696 process. Annu. Rev. Microbiol. 63, 311–34. doi:10.1146/annurev.micro.61.080706.093130
697 Kulm, L.D., Suess, E., Moore, J.C., Carson, B., Lewis, B.T., Ritger, S.D., Kadko, D.C.,
698 Thornbug, T.M., Embley, R.W., Rugh, W.D., Massoth, M.G., Langseth, Cochrane, G.R.,
699 Scamman, R.L., 1986. Oregon Subduction Zone: Venting, Fauna, and Carbonates. Science
700 (80-.). 231, 561–566.
701 Ladau, J., Sharpton, T.J., Finucane, M.M., Jospin, G., Kembel, S.W., O'Dwyer, J., Koeppel,
702 A.F., Green, J.L., Pollard, K.S., 2013. Global marine bacterial diversity peaks at high
703 latitudes in winter. ISME J. 7, 1669–77. doi:10.1038/ismej.2013.37
704 Levin, L.A., 2005. Ecology of Cold Seep Sediments: Interactions of fauna with flow, chemistry
705 and microbes 1–46.
706 Levin, L.A., Baco, A.R., Bowden, D., Colaço, A., Cordes, E., Cunha, M.R., Demopoulos, A.,
707 Gobin, J., Grupe, B., Le, J., Metaxas, A., Netburn, A., Rouse, G.W., Thurber, A.R.,
708 Tunnicliffe, V., Van Dover, C., Vanreusel, A., Watling, L., 2016. Hydrothermal Vents and
709 Methane Seeps: Rethinking the Sphere of Influence. Front. Mar. Sci. 3, 72.

710 doi:10.3389/fmars.2016.00072
711 Levin, L.A., Mendoza, G.F., Gonzalez, J.P., Thurber, A.R., Cordes, E.E., 2010. Diversity of
712 bathyal macrofauna on the northeastern Pacific margin: The influence of methane seeps and
713 oxygen minimum zones. Mar. Ecol. 31, 94–110. doi:10.1111/j.1439-0485.2009.00335.x
714 Levin, L.A., Sibuet, M., 2012. Understanding Continental Margin Biodiversity: A New
715 Imperative. Ann. Rev. Mar. Sci. 4, 79–112. doi:doi:10.1146/annurev-marine-120709-
716 142714
717 Lloyd, K.G., Albert, D.B., Biddle, J.F., Chanton, J.P., Pizarro, O., Teske, A., 2010. Spatial
718 structure and activity of sedimentary microbial communities underlying a Beggiatoa spp.
719 mat in a Gulf of Mexico hydrocarbon seep. PLoS One 5. doi:10.1371/journal.pone.0008738
720 Lösekann, T., Knittel, K., Nadalig, T., Fuchs, B., Niemann, H., Boetius, A., Amann, R., 2007.
721 Diversity and abundance of aerobic and anaerobic methane oxidizers at the Haakon Mosby
722 Mud Volcano, Barents Sea. Appl. Environ. Microbiol. 73, 3348–3362.
723 doi:10.1128/AEM.00016-07
724 Macalady, J.L., Dattagupta, S., Schaperdoth, I., Jones, D.S., Druschel, G.K., Eastman, D., 2008.
725 Niche differentiation among sulfur-oxidizing bacterial populations in cave waters. ISME J.
726 2, 590–601. doi:10.1038/ismej.2008.25
727 Marlow, J.J., Steele, J. a., Ziebis, W., Thurber, A.R., Levin, L. a., Orphan, V.J., 2014. Carbonate-
728 hosted methanotrophy represents an unrecognized methane sink in the deep sea. Nat.
729 Commun. 5, 5094. doi:10.1038/ncomms6094
730 Martiny, J.B.H., Bohannan, B.J.M., Brown, J.H., Kane, M., Krumins, J.A., Kuske, C.R., Morin,
731 P.J., Naeem, S., Øvreås, L., Reysenbach, A., Smith, V.H., 2006. Microbial biogeography :
732 putting microorganisms on the map 4, 102–113. doi:10.1038/nrmicro1341

733 Nguyen, P.M., 2016. Microbial sulfur transformations in novel laboratory-scale constructed
734 wetlands treating artificial wastewater. Helmholtz Cent. Environ. Res.
735 Orphan, V.J., Sylva, S.P., Hayes, J.M., Delong, E.F., 2001. Comparative Analysis of Methane-
736 Oxidizing Archaea and Sulfate-Reducing Bacteria in Anoxic Marine Sediments
737 Comparative Analysis of Methane-Oxidizing Archaea and Sulfate-Reducing Bacteria in
738 Anoxic Marine Sediments. Appl. Environ. Microbiol. 67, 1922–1934.
739 doi:10.1128/AEM.67.4.1922
740 Orphan, V.J., Ussler, W., Naehr, T.H., House, C.H., Hinrichs, K.U., Paull, C.K., 2004.
741 Geological, geochemical, and microbiological heterogeneity of the seafloor around methane
742 vents in the Eel River Basin, offshore California. Chem. Geol. 205, 265–289.
743 doi:10.1016/j.chemgeo.2003.12.035
744 Pasulka, A.L., Goffredi, S.K., Tavormina, P.L., Dawson, K.S., Levin, L.A., Rouse, G.W.,
745 Orphan, V.J., 2017. Colonial Tube-Dwelling Ciliates Influence Methane Cycling and
746 Microbial Diversity within Methane Seep Ecosystems. Front. Mar. Sci. 3, 1–17.
747 doi:10.3389/fmars.2016.00276
748 Pasulka, A.L., Levin, L.A., Steele, J.A., Case, D.H., Landry, M.R., Orphan, V.J., 2016.
749 Microbial eukaryotic distributions and diversity patterns in a deep-sea methane seep
750 ecosystem. Environ. Microbiol. 18, 3022–3043. doi:10.1111/1462-2920.13185
751 Pjevac, P., 2014. Co-existence and niche differentiation of sulfur oxidizing bacteria in marine
752 environments.
753 Ritt, B., Pierre, C., Gauthier, O., Wenzhöfer, F., Boetius, A., Sarrazin, J., 2011. Diversity and
754 distribution of cold-seep fauna associated with different geological and environmental
755 settings at mud volcanoes and pockmarks of the Nile Deep-Sea Fan. Mar. Biol. 158, 1187.

doi:10.1007/s00227-011-1679-6

Ruff, S.E., Biddle, J.F., Teske, A.P., Knittel, K., Boetius, A., Ramette, A., 2015. Global dispersion and local diversification of the methane seep microbiome 112, 4015–4020. doi:10.1073/pnas.1421865112

Ruff, S.E., Kuhfuss, H., Wegener, G., Lott, C., Ramette, A., Wiedling, J., Knittel, K., Weber, M., 2016. Methane seep in shallow-water permeable sediment harbors high diversity of anaerobic methanotrophic communities, Elba, Italy. Front. Microbiol. 7, 1–20. doi:10.3389/fmicb.2016.00374

Sahling, H., Rickert, D., Lee, R.W., Linke, P., Suess, E., 2002. Macrofaunal community structure and sulfide flux at gas hydrate deposits from the Cascadia convergent margin, NE Pacific. Mar. Ecol. Prog. Ser. 231, 121–138. doi:10.3354/meps231121

Schloss, P.D., Gevers, D., Westcott, S.L., 2011. Reducing the effects of PCR amplification and sequencing Artifacts on 16s rRNA-based studies. PLoS One 6. doi:10.1371/journal.pone.0027310

Smith, W.F., Sandwell, D.T., 1997. Global sea floor topography from satellite altimetry and ship depth soundings. Science 277 (5334), 1956–1962

Sweetman, A.K., Thurber, A.R., Smith, C.R., Levin, L.A., Mora, C., Wei, C.-L., Gooday, A.J., Jones, D.O.B., Rex, M., Yasuhara, M., Ingels, J., Ruhl, H.A., Frieder, C.A., Danovaro, R., Würzberg, L., Baco, A., Grupe, B.M., Pasulka, A., Meyer, K.S., Dunlop, K.M., Henry, L.-A., Roberts, J.M., 2017. Major impacts of climate change on deep-sea benthic ecosystems. Elem Sci Anth 5, 4. doi:10.1525/elementa.203

Thurber, A.R., Sweetman, A.K., Narayanaswamy, B.E., Jones, D.O.B., Ingels, J., Hansman, R.L., 2014. Ecosystem function and services provided by the deep sea. Biogeosciences 11,

779 3941–3963. doi:10.5194/bg-11-3941-2014
780 Torres, M.E., Teichert, B.M.A., Tréhu, A.M., Borowski, W., Tomaru, H., 2004. Relationship of
781 pore water freshening to accretionary processes in the Cascadia margin: Fluid sources and
782 gas hydrate abundance. Geophys. Res. Lett. 31, 1–4. doi:10.1029/2004GL021219
783 Tréhu, A.M., Torres, M.E., Moore, G.F., Suess, E., Bohrmann, G., 1999. Temporal and spatial
784 evolution of a gas hydrate-bearing accretionary ridge on the Oregon continental margin.
785 Geology 27, 939–942. doi:10.1130/0091-7613(1999)027<0939:TASEOA>2.3.CO;2
786 Tryon, M.D., Brown, K.M., Torres, M.E., 2002. Fluid and chemical flux in and out of sediments
787 hosting methane hydrate deposits on Hydrate Ridge, OR, II: Hydrological processes. Earth
788 Planet. Sci. Lett. 201, 541–557. doi:10.1016/S0012-821X(02)00732-X
789 Tryon, M.D., Brown, K.M., Torres, M.E., Tréhu, A.M., McManus, J., Collier, R.W., 1999.
790 Measurements of transience and downward fluid flow near episodic methane gas vents,
791 Hydrate Ridge, Cascadia. Geology 27, 1075–1078. doi:10.1130/0091-
792 7613(1999)027<1075:MOTADF>2.3.CO;2
793 Valentine, D.L., 2011. Emerging topics in marine methane biogeochemistry. Ann. Rev. Mar. Sci.
794 3, 147–171. doi:10.1146/annurev-marine-120709-142734
795 Valentine, D.L., Kastner, M., Wardlaw, G.D., Wang, X., Purdy, A., Bartlett, D.H., 2005.
796 Biogeochemical investigations of marine methane seeps, Hydrate Ridge, Oregon. J.
797 Geophys. Res. 110, G02005. doi:10.1029/2005JG000025
798 Van Dover, C.L., German, C.R., Speer, K.G., Parson, L.M., Vrijenhoek, R.C., 2002. Evolution
799 and biogeography of deep-sea vent and seep invertebrates. Science (80-.). 295, 1253–1257.
800 doi:10.1126/science.1067361
801 Wallmann, K., Linke, P., Suess, E., Bohrmann, G., Sahling, H., Schlüter, M., Dählmann, A.,

802 Lammers, S., Greinert, J., von Mirbach, N., 1997. Quantifying fluid flow, solute mixing,
803 and biogeochemical turnover at cold vents of the eastern Aleutian subduction zone.
804 Geochim. Cosmochim. Acta 61, 5209–5219. doi:10.1016/S0016-7037(97)00306-2
805 Yamaguchi, T., Newman, W.A., Hashimoto, J., 2004. A cold seep barnacle (Cirripedia :
806 Neolepadinae) from Japan and the age of the vent/seep fauna. J. Mar. Biol. Assoc. United
807 Kingdom 84, 111–120. doi:10.1017/S0025315404008975h
808

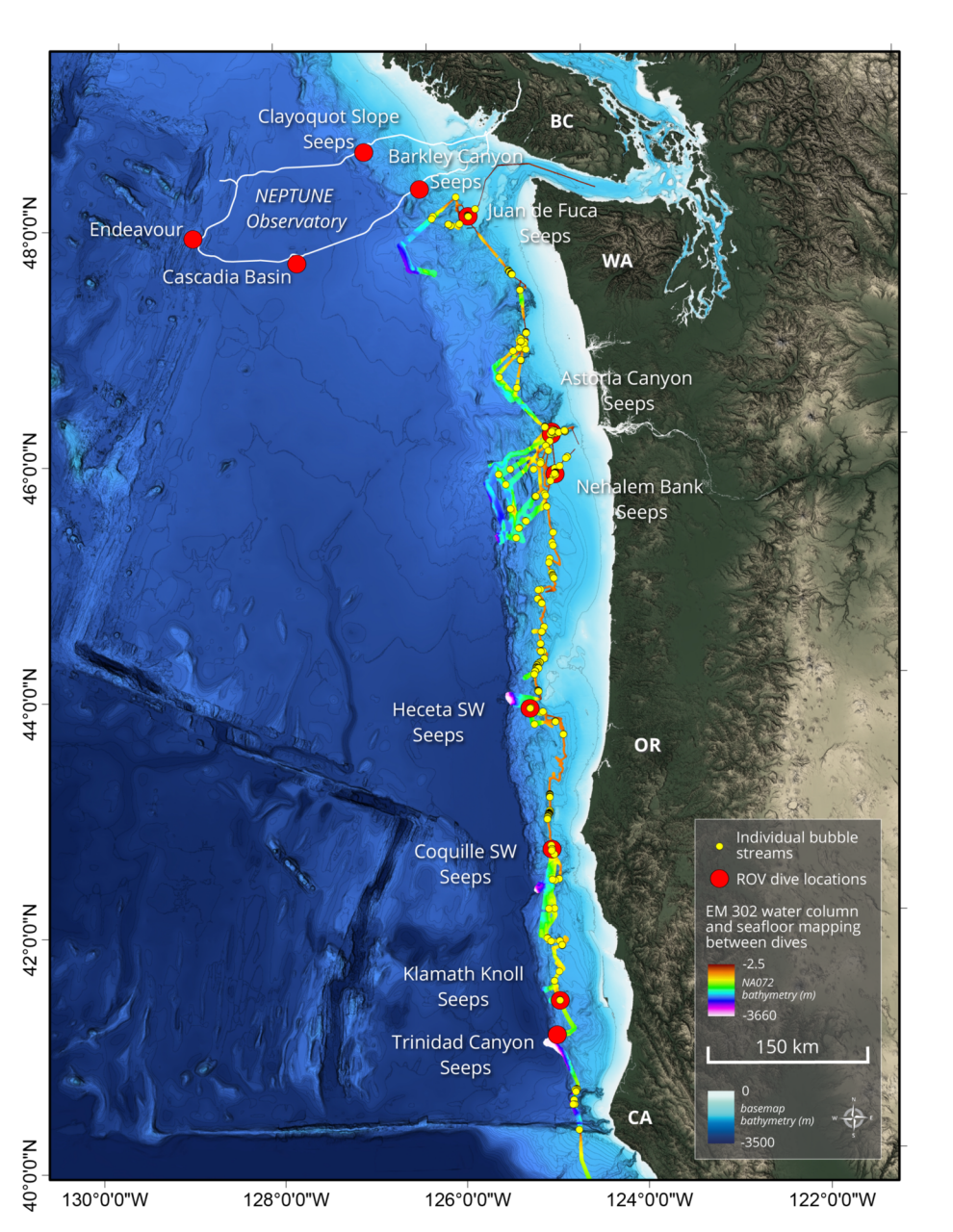
Clayoquot Slope Seeps
Barkley Canyon Seeps
NEPTUNE Observatory
Endeavour
Cascadia Basin
Juan de Fuca Seeps
BC
WA
Astoria Canyon Seeps
Nehalem Bank Seeps
Heceta SW Seeps
OR
Coquille SW Seeps
Klamath Knoll Seeps
Trinidad Canyon Seeps
CA
48°0'0"N
46°0'0"N
44°0'0"N
42°0'0"N
40°0'0"N
130°0'0"W
128°0'0"W
126°0'0"W
124°0'0"W
122°0'0"W
Individual bubble streams
ROV dive locations
EM 302 water column and seafloor mapping between dives
-2.5
NA072 bathymetry (m)
-3660
150 km
0
basemap bathymetry (m)
-3500

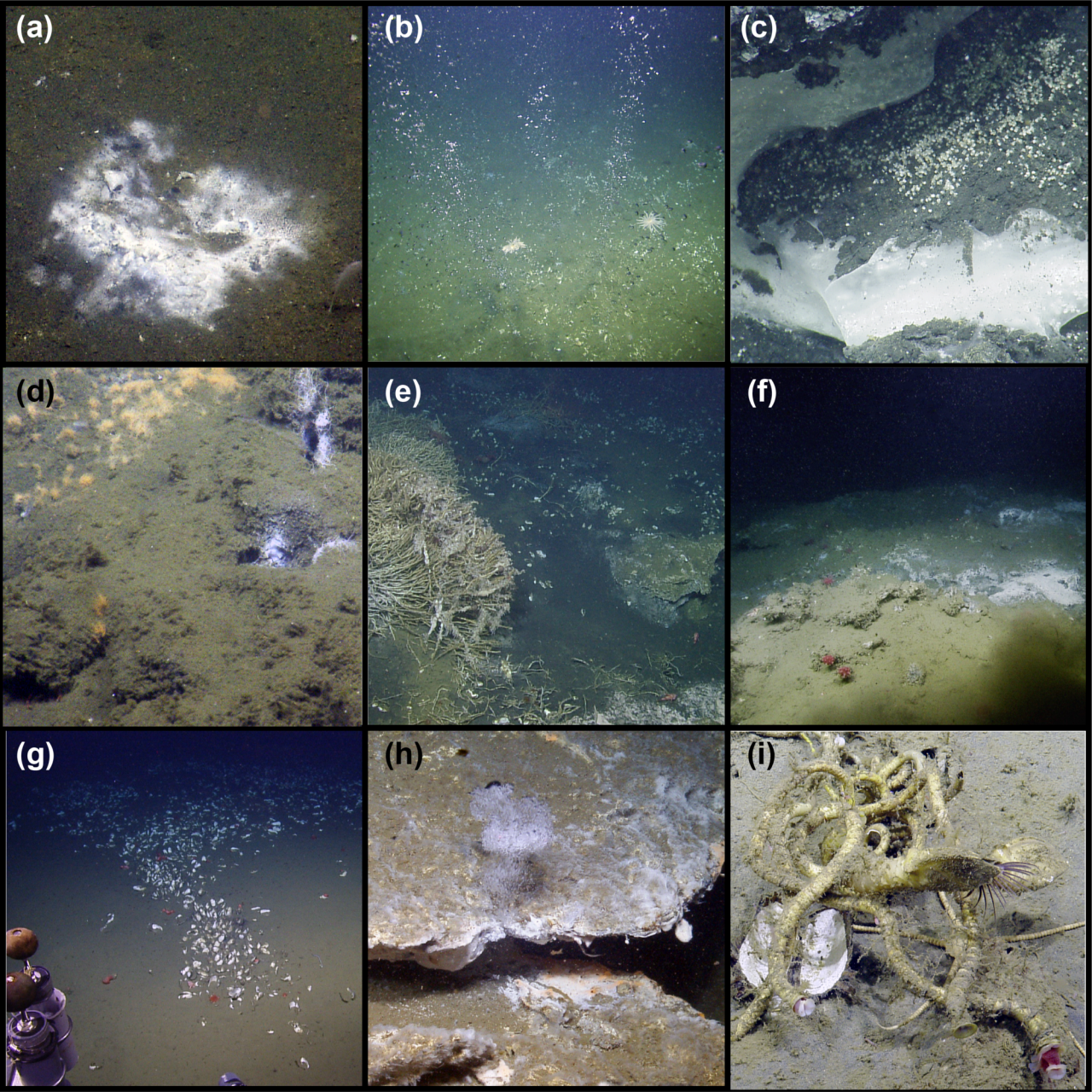
(a)
(b)
(c)
(d)
(e)
(f)
(g)
(h)
(i)

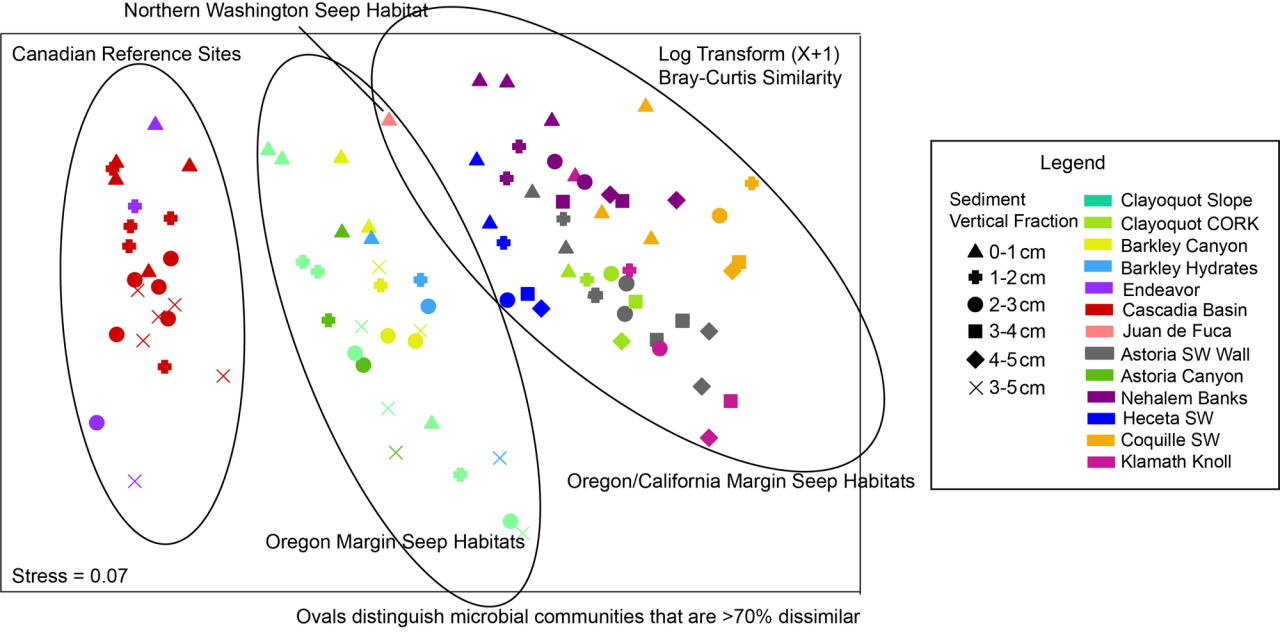
Northern Washington Seep Habitat
Canadian Reference Sites
Log Transform (X+1)
Bray-Curtis Similarity
Oregon/California Margin Seep Habitats
Oregon Margin Seep Habitats
Stress = 0.07
Ovals distinguish microbial communities that are >70% dissimilar
Legend
Sediment
Vertical Fraction
0-1 cm
1-2 cm
2-3 cm
3-4 cm
4-5 cm
3-5 cm
Clayoquot Slope
Clayoquot CORK
Barkley Canyon
Barkley Hydrates
Endeavor
Cascadia Basin
Juan de Fuca
Astoria SW Wall
Astoria Canyon
Nehalem Banks
Heceta SW
Coquille SW
Klamath Knoll

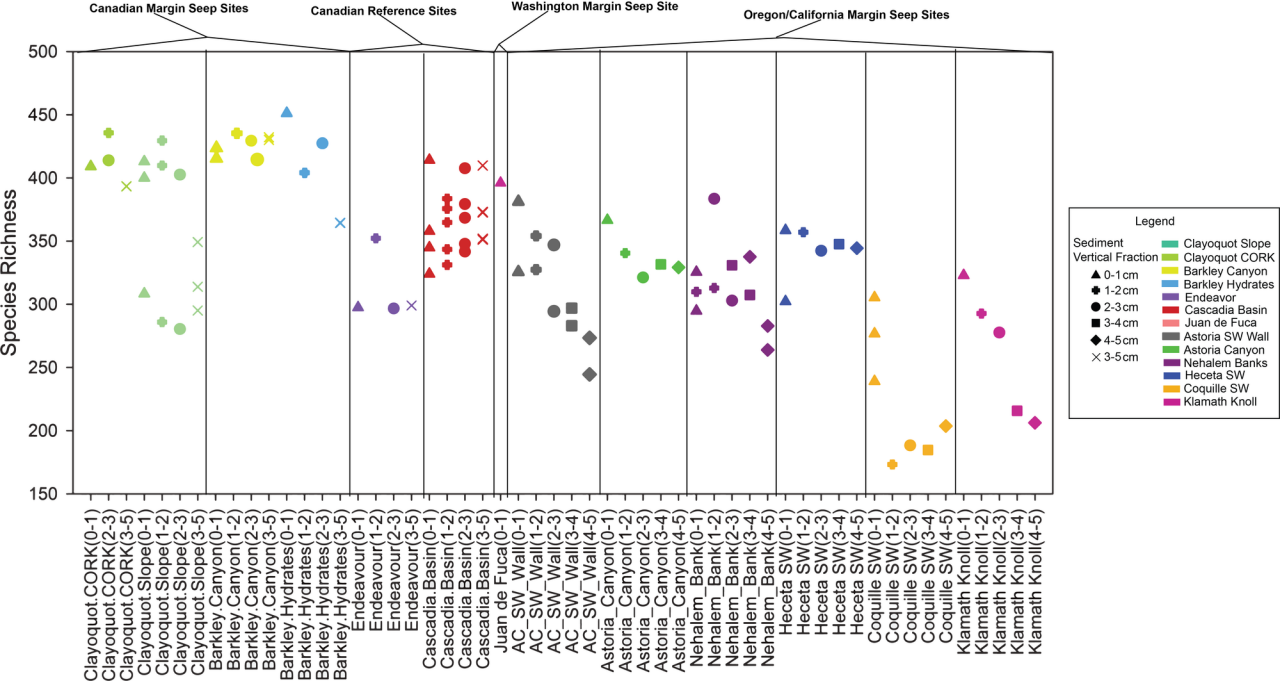
Canadian Margin Seep Sites
Canadian Reference Sites
Washington Margin Seep Site
Oregon/California Margin Seep Sites
Species Richness
500
450
400
350
300
250
200
150
Clayoquot.CORK(0-1)
Clayoquot.CORK(2-3)
Clayoquot.CORK(3-5)
Clayoquot.Slope(0-1)
Clayoquot.Slope(1-2)
Clayoquot.Slope(2-3)
Clayoquot.Slope(3-5)
Barkley.Canyon(0-1)
Barkley.Canyon(1-2)
Barkley.Canyon(2-3)
Barkley.Canyon(3-5)
Barkley.Hydrates(0-1)
Barkley.Hydrates(1-2)
Barkley.Hydrates(2-3)
Barkley.Hydrates(3-5)
Endeavour(0-1)
Endeavour(1-2)
Endeavour(2-3)
Endeavour(3-5)
Cascadia.Basin(0-1)
Cascadia.Basin(1-2)
Cascadia.Basin(2-3)
Cascadia.Basin(3-5)
Juan de Fuca(0-1)
AC_SW_Wall(0-1)
AC_SW_Wall(1-2)
AC_SW_Wall(2-3)
AC_SW_Wall(3-4)
AC_SW_Wall(4-5)
Astoria_Canyon(0-1)
Astoria_Canyon(1-2)
Astoria_Canyon(2-3)
Astoria_Canyon(3-4)
Astoria_Canyon(4-5)
Nehalem_Bank(0-1)
Nehalem_Bank(1-2)
Nehalem_Bank(2-3)
Nehalem_Bank(3-4)
Nehalem_Bank(4-5)
Heceta SW(0-1)
Heceta SW(1-2)
Heceta SW(2-3)
Heceta SW(3-4)
Heceta SW(4-5)
Coquille SW(0-1)
Coquille SW(1-2)
Coquille SW(2-3)
Coquille SW(3-4)
Coquille SW(4-5)
Klamath Knoll(0-1)
Klamath Knoll(1-2)
Klamath Knoll(2-3)
Klamath Knoll(3-4)
Klamath Knoll(4-5)
Legend
Sediment Vertical Fraction
0-1cm
1-2cm
2-3cm
3-4cm
4-5cm
3-5cm
Clayoquot Slope
Clayoquot CORK
Barkley Canyon
Barkley Hydrates
Endeavor
Cascadia Basin
Juan de Fuca
Astoria SW Wall
Astoria Canyon
Nehalem Banks
Heceta SW
Coquille SW
Klamath Knoll

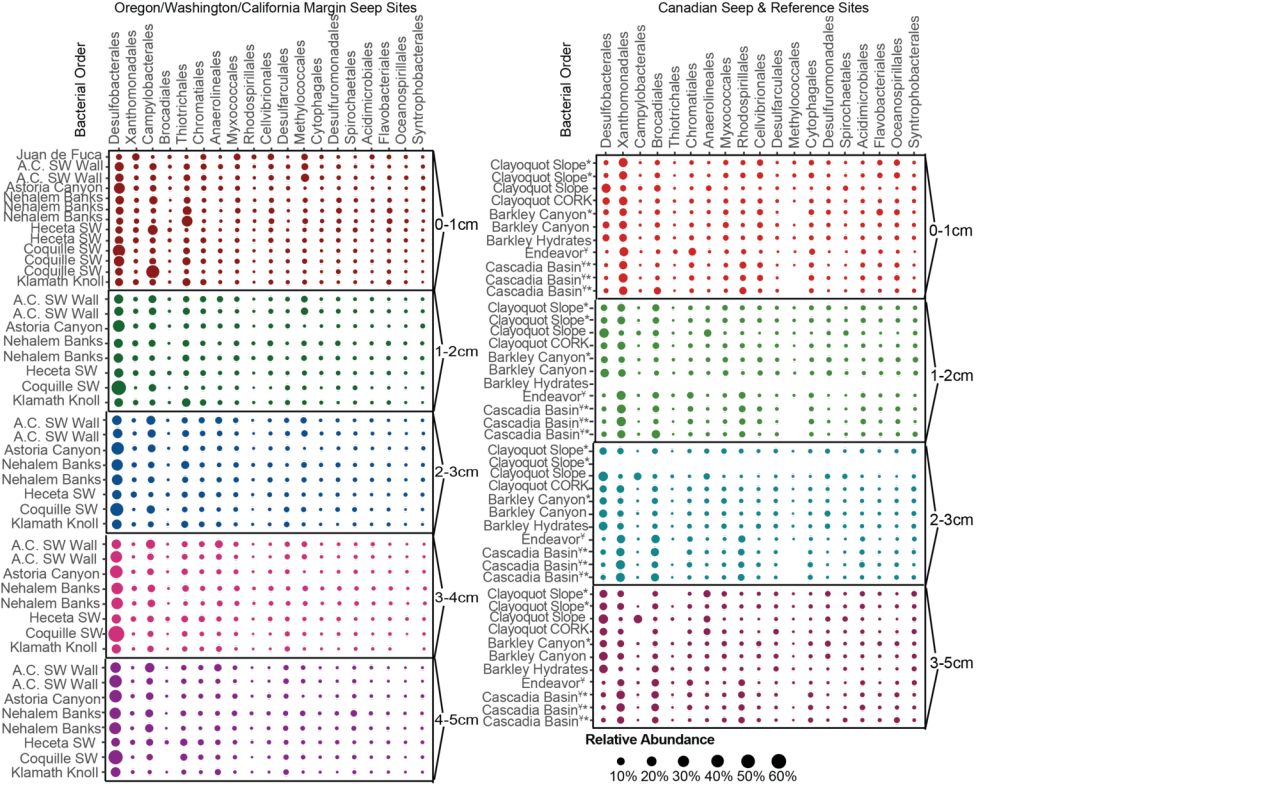
Oregon/Washington/California Margin Seep Sites
Bacterial Order
Desulfobacterales
Xanthomonadales
Campylobacterales
Brocadiales
Thiotrichales
Chromatiales
Anaerolineales
Myxococcales
Rhodospirillales
Cellvibrionales
Desulfarculales
Methylococcales
Cytophagales
Desulfuromonadales
Spirochaetales
Acidimicrobiales
Flavobacteriales
Oceanospirillales
Syntrophobacterales
Juan de Fuca
A.C. SW Wall
A.C. SW Wall
Astoria Canyon
Nehalem Banks
Nehalem Banks
Nehalem Banks
Heceta SW
Heceta SW
Coquille SW
Coquille SW
Coquille SW
Klamath Knoll
0-1cm
1-2cm
2-3cm
3-4cm
4-5cm
Canadian Seep & Reference Sites
Bacterial Order
Desulfobacterales
Xanthomonadales
Campylobacterales
Brocadiales
Thiotrichales
Chromatiales
Anaerolineales
Myxococcales
Rhodospirillales
Cellvibrionales
Desulfarculales
Methylococcales
Cytophagales
Desulfuromonadales
Spirochaetales
Acidimicrobiales
Flavobacteriales
Oceanospirillales
Syntrophobacterales
Clayoquot Slope*
Clayoquot Slope*
Clayoquot Slope
Clayoquot CORK
Barkley Canyon*
Barkley Canyon
Barkley Hydrates
Endeavor*
Cascadia Basin**
Cascadia Basin**
Cascadia Basin**
0-1cm
1-2cm
2-3cm
3-5cm
Relative Abundance
10% 20% 30% 40% 50% 60%

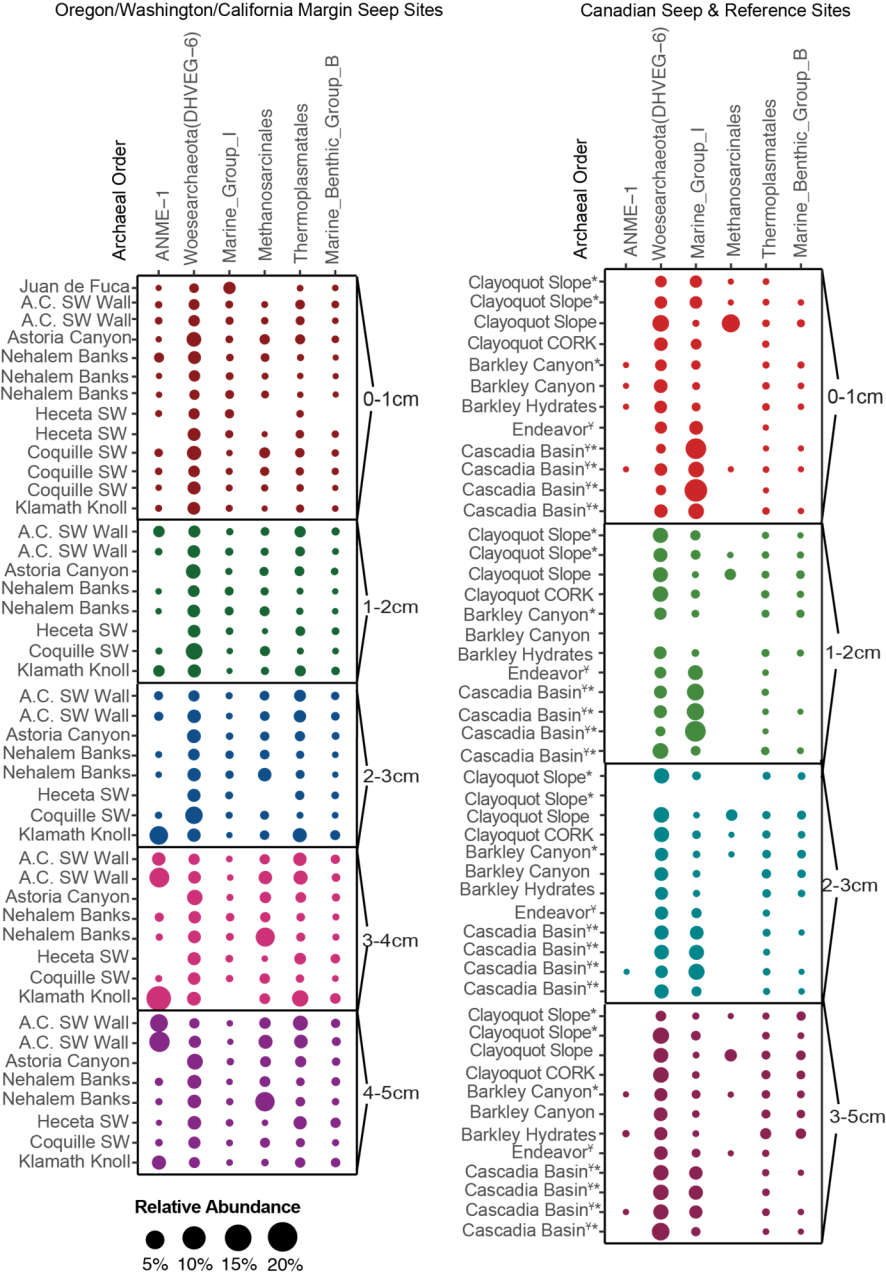
Oregon/Washington/California Margin Seep Sites
Canadian Seep & Reference Sites
Archaeal Order
ANME−1
Woesearchaeota(DHVEG−6)
Marine_Group_I
Methanosarcinales
Thermoplasmatales
Marine_Benthic_Group_B
Juan de Fuca
A.C. SW Wall
A.C. SW Wall
Astoria Canyon
Nehalem Banks
Nehalem Banks
Nehalem Banks
Heceta SW
Heceta SW
Coquille SW
Coquille SW
Coquille SW
Klamath Knoll
0-1cm
A.C. SW Wall
A.C. SW Wall
Astoria Canyon
Nehalem Banks
Nehalem Banks
Heceta SW
Coquille SW
Klamath Knoll
1-2cm
A.C. SW Wall
A.C. SW Wall
Astoria Canyon
Nehalem Banks
Nehalem Banks
Heceta SW
Coquille SW
Klamath Knoll
2-3cm
A.C. SW Wall
A.C. SW Wall
Astoria Canyon
Nehalem Banks
Nehalem Banks
Heceta SW
Coquille SW
Klamath Knoll
3-4cm
A.C. SW Wall
A.C. SW Wall
Astoria Canyon
Nehalem Banks
Nehalem Banks
Heceta SW
Coquille SW
Klamath Knoll
4-5cm
Relative Abundance
5%
10%
15%
20%
Clayoquot Slope*
Clayoquot Slope*
Clayoquot Slope
Clayoquot CORK
Barkley Canyon*
Barkley Canyon
Barkley Hydrates
Endeavor¥
Cascadia Basin¥*
Cascadia Basin¥*
Cascadia Basin¥*
Cascadia Basin¥*
0-1cm
Clayoquot Slope*
Clayoquot Slope*
Clayoquot Slope
Clayoquot CORK
Barkley Canyon*
Barkley Canyon
Barkley Hydrates
Endeavor¥
Cascadia Basin¥*
Cascadia Basin¥*
Cascadia Basin¥*
Cascadia Basin¥*
1-2cm
Clayoquot Slope*
Clayoquot Slope*
Clayoquot Slope
Clayoquot CORK
Barkley Canyon*
Barkley Canyon
Barkley Hydrates
Endeavor¥
Cascadia Basin¥*
Cascadia Basin¥*
Cascadia Basin¥*
Cascadia Basin¥*
2-3cm
Clayoquot Slope*
Clayoquot Slope*
Clayoquot Slope
Clayoquot CORK
Barkley Canyon*
Barkley Canyon
Barkley Hydrates
Endeavor¥
Cascadia Basin¥*
Cascadia Basin¥*
Cascadia Basin¥*
Cascadia Basin¥*
3-5cm

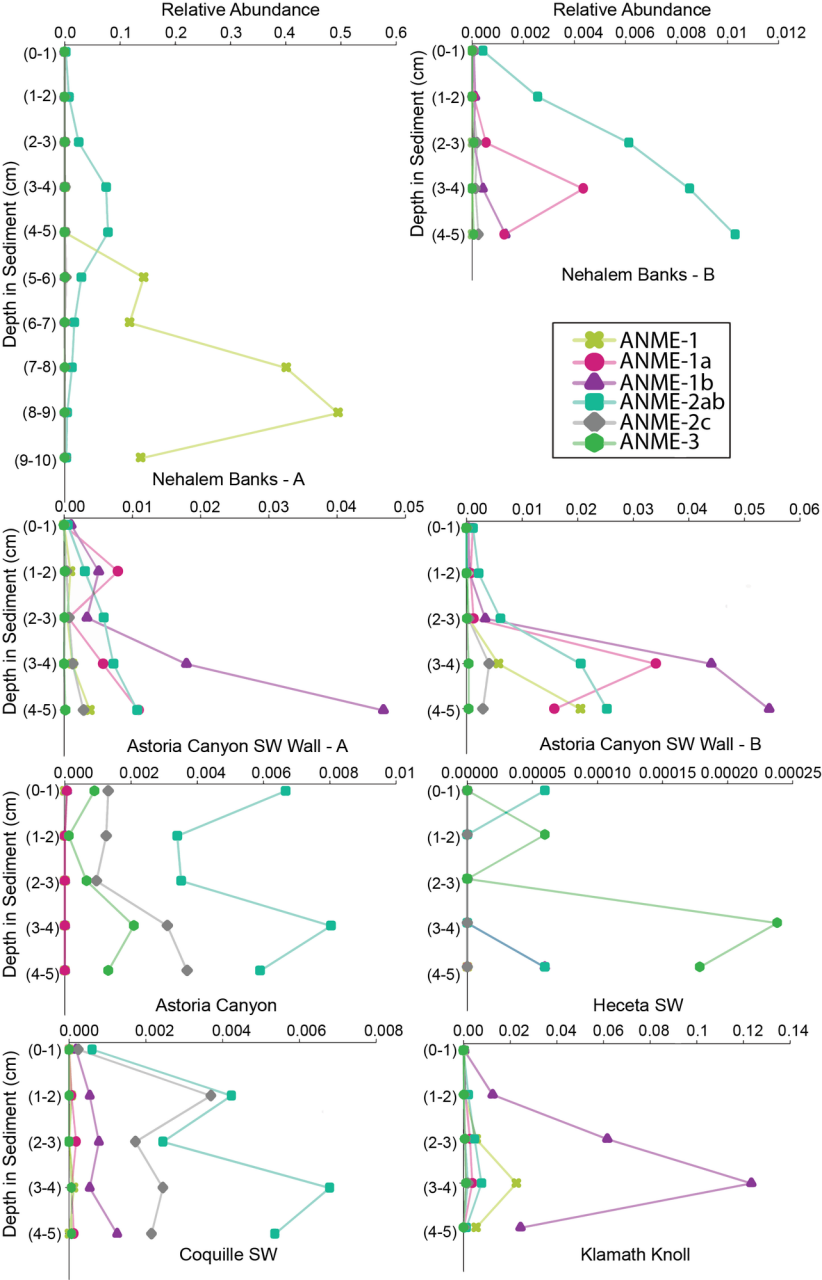
Relative Abundance
Depth in Sediment (cm)
(0-1)
(1-2)
(2-3)
(3-4)
(4-5)
(5-6)
(6-7)
(7-8)
(8-9)
(9-10)
Nehalem Banks - A
Nehalem Banks - B
ANME-1
ANME-1a
ANME-1b
ANME-2ab
ANME-2c
ANME-3
Astoria Canyon SW Wall - A
Astoria Canyon SW Wall - B
Astoria Canyon
Heceta SW
Coquille SW
Klamath Knoll

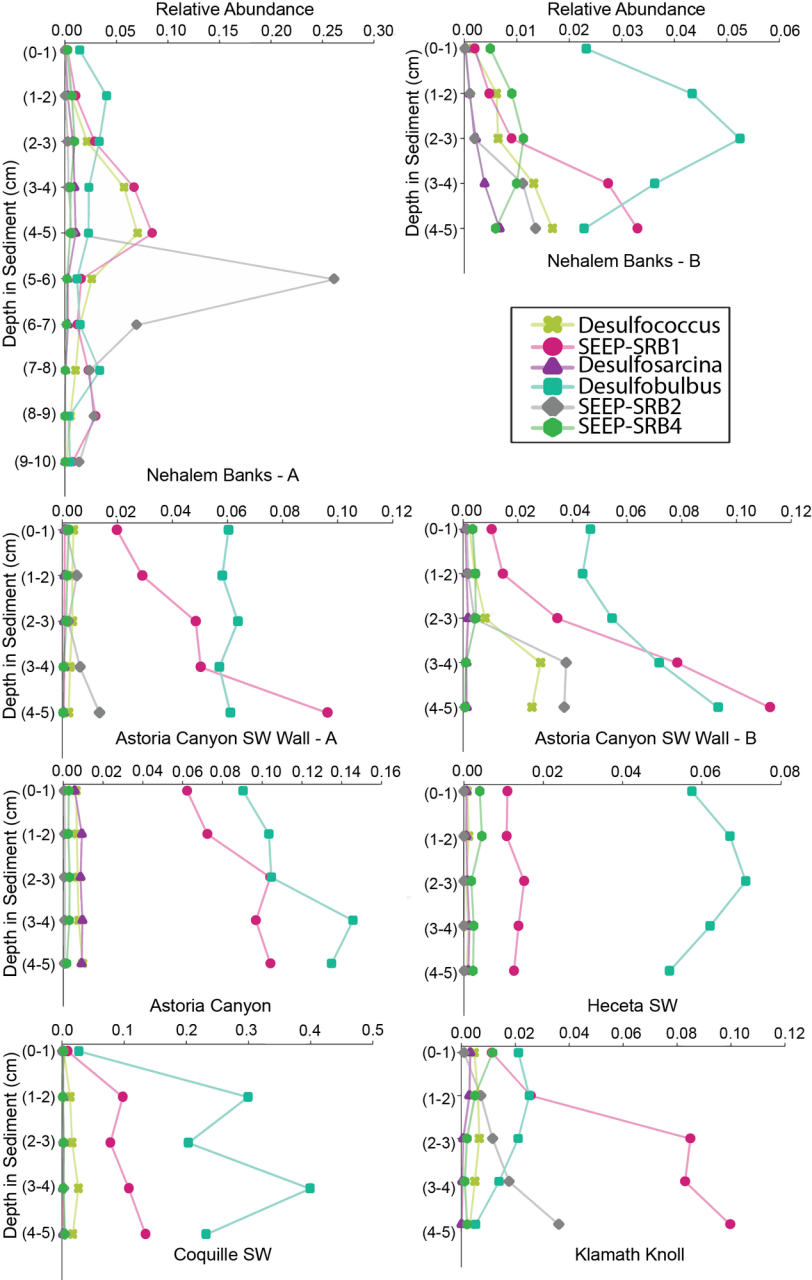
Relative Abundance
0.00
0.05
0.10
0.15
0.20
0.25
0.30
Depth in Sediment (cm)
(0-1)
(1-2)
(2-3)
(3-4)
(4-5)
(5-6)
(6-7)
(7-8)
(8-9)
(9-10)
Nehalem Banks - A
Relative Abundance
0.00
0.01
0.02
0.03
0.04
0.05
0.06
Depth in Sediment (cm)
(0-1)
(1-2)
(2-3)
(3-4)
(4-5)
Nehalem Banks - B
Desulfococcus
SEEP-SRB1
Desulfosarcina
Desulfobulbus
SEEP-SRB2
SEEP-SRB4
0.00
0.02
0.04
0.06
0.08
0.10
0.12
Depth in Sediment (cm)
(0-1)
(1-2)
(2-3)
(3-4)
(4-5)
Astoria Canyon SW Wall - A
0.00
0.02
0.04
0.06
0.08
0.10
0.12
Depth in Sediment (cm)
(0-1)
(1-2)
(2-3)
(3-4)
(4-5)
Astoria Canyon SW Wall - B
0.00
0.02
0.04
0.06
0.08
0.10
0.12
0.14
0.16
Depth in Sediment (cm)
(0-1)
(1-2)
(2-3)
(3-4)
(4-5)
Astoria Canyon
0.00
0.02
0.04
0.06
0.08
Depth in Sediment (cm)
(0-1)
(1-2)
(2-3)
(3-4)
(4-5)
Heceta SW
0.0
0.1
0.2
0.3
0.4
0.5
Depth in Sediment (cm)
(0-1)
(1-2)
(2-3)
(3-4)
(4-5)
Coquille SW
0.00
0.02
0.04
0.06
0.08
0.10
0.12
Depth in Sediment (cm)
(0-1)
(1-2)
(2-3)
(3-4)
(4-5)
Klamath Knoll

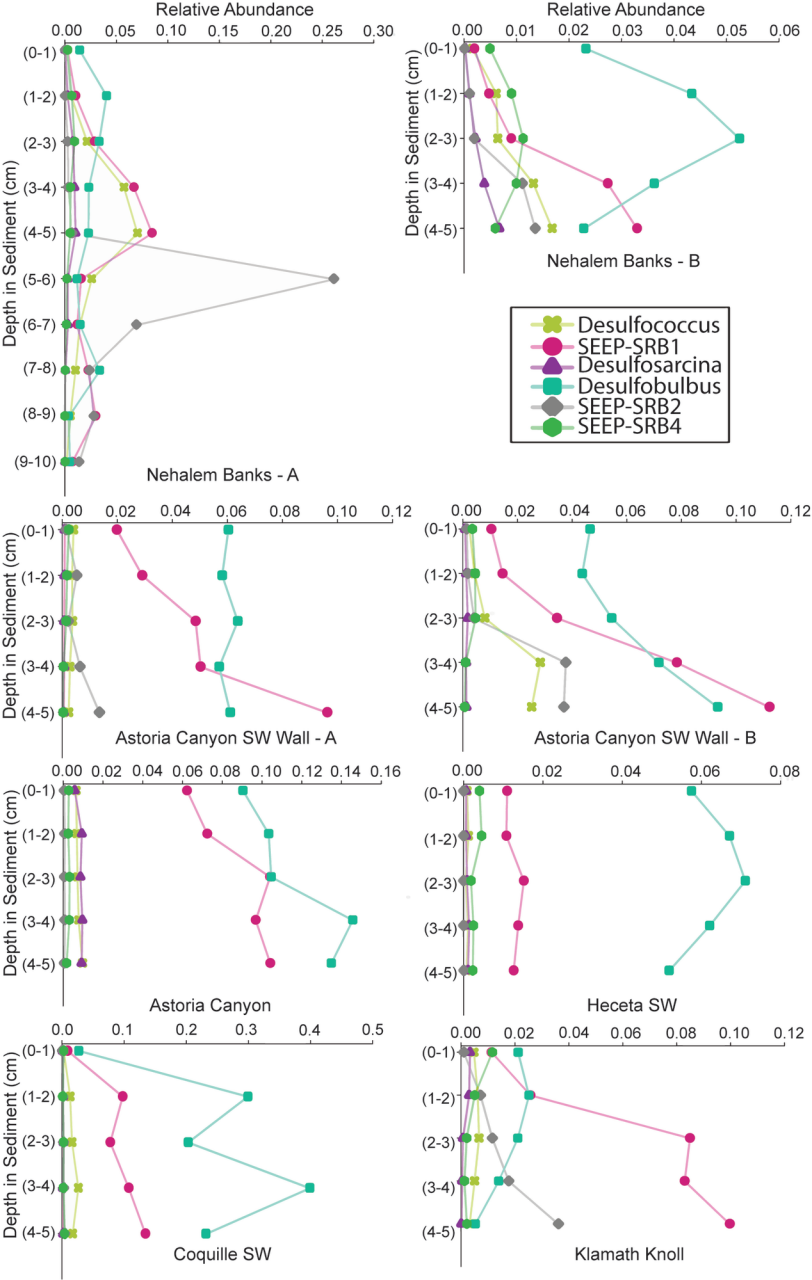
Relative Abundance
0.00 0.05 0.10 0.15 0.20 0.25 0.30
Depth in Sediment (cm)
(0-1)
(1-2)
(2-3)
(3-4)
(4-5)
(5-6)
(6-7)
(7-8)
(8-9)
(9-10)
Nehalem Banks - A
Relative Abundance
0.00 0.01 0.02 0.03 0.04 0.05 0.06
Depth in Sediment (cm)
(0-1)
(1-2)
(2-3)
(3-4)
(4-5)
Nehalem Banks - B
Desulfococcus
SEEP-SRB1
Desulfosarcina
Desulfobulbus
SEEP-SRB2
SEEP-SRB4
0.00 0.02 0.04 0.06 0.08 0.10 0.12
Depth in Sediment (cm)
(0-1)
(1-2)
(2-3)
(3-4)
(4-5)
Astoria Canyon SW Wall - A
0.00 0.02 0.04 0.06 0.08 0.10 0.12
(0-1)
(1-2)
(2-3)
(3-4)
(4-5)
Astoria Canyon SW Wall - B
0.00 0.02 0.04 0.06 0.08 0.10 0.12 0.14 0.16
Depth in Sediment (cm)
(0-1)
(1-2)
(2-3)
(3-4)
(4-5)
Astoria Canyon
0.00 0.02 0.04 0.06 0.08
(0-1)
(1-2)
(2-3)
(3-4)
(4-5)
Heceta SW
0.0 0.1 0.2 0.3 0.4 0.5
Depth in Sediment (cm)
(0-1)
(1-2)
(2-3)
(3-4)
(4-5)
Coquille SW
0.00 0.02 0.04 0.06 0.08 0.10 0.12
(0-1)
(1-2)
(2-3)
(3-4)
(4-5)
Klamath Knoll

Table 1: Sampling sites off the Washington/Oregon/California Margin, 40-48°N, during E/V *Nautilus* cruise NA072 and off of British Columbia, Canada), 47-49°N, during TG Thompson (TN328), and E/V Nautilus (NA071) cruises.

Cruise Number	Date Sampled	Site	Latitude (N)	Longitude (W)	Depth (m)	Temperature (˚C)	Oxygen (µmol /L)	Habitat description
NA072	June 2016	Juan de Fuca	48.1015	-125.5544	150	6.67	90.48	Microbial mats*
NA072	June 2016	Nehalem Bank	45.8837	-124.6434	190	6.75	66.61	Microbial mats (orange and white)*
NA072	June 2016	Astoria Canyon	46.2422	-124.6494	850	3.76	4.78	Microbial mats*, polychaete beds, exposed hydrates, pockmarks
NA072	June 2016	Astoria Canyon SW wall	46.2224	-124.6564	495	5.02	24.46	Clam beds*,authigenic carbonates
NA072	June 2016	Heceta SW	43.9109	-125.0756	1225	3.05	16.26	Siboglinidae assemblages*, microbial mats*, clam beds* polychaete beds, polychaete beds, authigenic carbonates, exposed hydrates, pockmarks
NA072	June 2016	Coquille SW	42.7107	-124.9011	615	4.61	7.43	Microbial mats*, clam beds*, authigenic carbonates
NA072	June 2016	Klamath Knoll	41.4274	-124.8917	735	4.07	5.27	Clam beds*, microbial mats (orange and white), authigenic carbonates
NA072	June 2016	Trinidad Canyon[2]	41.1385	-124.9443	2149	1.98	56.90	Siboglindae assemblages, gooseneck barnacles, live and dead clam bed assemblages, patches of reduced sediment, authigenic carbonates
TN328, NA071	Sept 2015, May 2016	Clayoquot Slope	48.6707	-126.8478	1250	2.85	13.4-22.3	Muddy sediments*, methane gas, bubbles, extensive microbial mats, clam beds*, methane gas hydrates
TN328, NA071	Sept 2015, May 2016	Barkley Canyon	48.3166	-126.0508	985	3.61	6.7-13.4	Muddy sediments*, microbial mats, methane gas hydrates, exposed hydrate mounds, clam beds
NA071	May 2016	Endeavour	47.9493	-129.0983	2300	2.47	54.46	Mid-Ocean Ridge; Hydrothermal vent field rich with fissures, pillow lava deposits sulphide towers, rocky outcrops, fine grained sediment*
TN328	May 2015	Cascadia Basin	47.7627	-127.7589	2660	1.78	72.56	Abyssal Plain; Fine-grained sediment*

* Indicates habitat sediment core was taken from

[2] Not sampled